Evaluating Model Simulations of Twentieth-Century Sea Level Rise. Part I: Global Mean Sea Level Change

AIMÉE B. A. SLANGEN,[a] BENOIT MEYSSIGNAC,[b] CECILE AGOSTA,[c] NICOLAS CHAMPOLLION,[d] JOHN A. CHURCH,[e] XAVIER FETTWEIS,[c] STEFAN R. M. LIGTENBERG,[f] BEN MARZEION,[g] ANGELIQUE MELET,[h] MATTHEW D. PALMER,[i] KRISTIN RICHTER,[j] CHRISTOPHER D. ROBERTS,[i,k] AND GIORGIO SPADA[l]

[a] *Department of Estuarine and Delta Systems, Royal Netherlands Institute for Sea Research (NIOZ), and Utrecht University, Yerseke, Netherlands*
[b] *LEGOS, Université de Toulouse, CNES, CNRS, IRD, UPS, Toulouse, France*
[c] *Département de Géographie, Université de Liège, Belgium*
[d] *International Space Science Institute, Bern, Switzerland*
[e] *Climate Change Research Centre, University of New South Wales, Sydney, New South Wales, Australia*
[f] *Institute for Marine and Atmospheric Research, Utrecht University, Utrecht, Netherlands*
[g] *Institute of Geography, University of Bremen, Bremen, Germany*
[h] *Mercator Ocean, Ramonville-Saint-Agne, France*
[i] *Met Office Hadley Centre, Exeter, United Kingdom*
[j] *Institute of Atmospheric and Cryospheric Sciences, University of Innsbruck, Innsbruck, Austria*
[k] *European Centre for Medium-Range Weather Forecasts, Shinfield, United Kingdom*
[l] *Dipartimento di Scienze Pure e Applicate, Urbino University "Carlo Bo," Urbino, Italy*

(Manuscript received 23 February 2017, in final form 28 June 2017)

ABSTRACT

Sea level change is one of the major consequences of climate change and is projected to affect coastal communities around the world. Here, global mean sea level (GMSL) change estimated by 12 climate models from phase 5 of the World Climate Research Programme's Climate Model Intercomparison Project (CMIP5) is compared to observational estimates for the period 1900–2015. Observed and simulated individual contributions to GMSL change (thermal expansion, glacier mass change, ice sheet mass change, landwater storage change) are analyzed and compared to observed GMSL change over the period 1900–2007 using tide gauge reconstructions, and over the period 1993–2015 using satellite altimetry estimates. The model-simulated contributions explain 50% ± 30% (uncertainties 1.65σ unless indicated otherwise) of the mean observed change from 1901–20 to 1988–2007. Based on attributable biases between observations and models, a number of corrections are proposed, which result in an improved explanation of 75% ± 38% of the observed change. For the satellite era (from 1993–97 to 2011–15) an improved budget closure of 102% ± 33% is found (105% ± 35% when including the proposed bias corrections). Simulated decadal trends increase over the twentieth century, both in the thermal expansion and the combined mass contributions (glaciers, ice sheets, and landwater storage). The mass components explain the majority of sea level rise over the twentieth century, but the thermal expansion has increasingly contributed to sea level rise, starting from 1910 onward and in 2015 accounting for 46% of the total simulated sea level change.

1. Introduction

Sea level change is one of the most well-known consequences of climate change, affecting coastal communities and ecosystems worldwide. Changes in sea level are the result of changes in different components of the climate system: the ocean, the land, the atmosphere, and the cryosphere. Therefore, the study of sea level change is like a jigsaw puzzle, requiring a complete and integrative view of the climate system on a range of spatial and temporal scales (Fig. 1; Church et al. 2013a; Cazenave et al. 2017).

On a global scale, there are several processes that contribute to long-term sea level change. A major process is the thermal expansion and contraction of the ocean water, caused by density changes due to temperature

Denotes content that is immediately available upon publication as open access.

Corresponding author: Aimée B. A. Slangen, aimee.slangen@gmail.com.

DOI: 10.1175/JCLI-D-17-0110.1

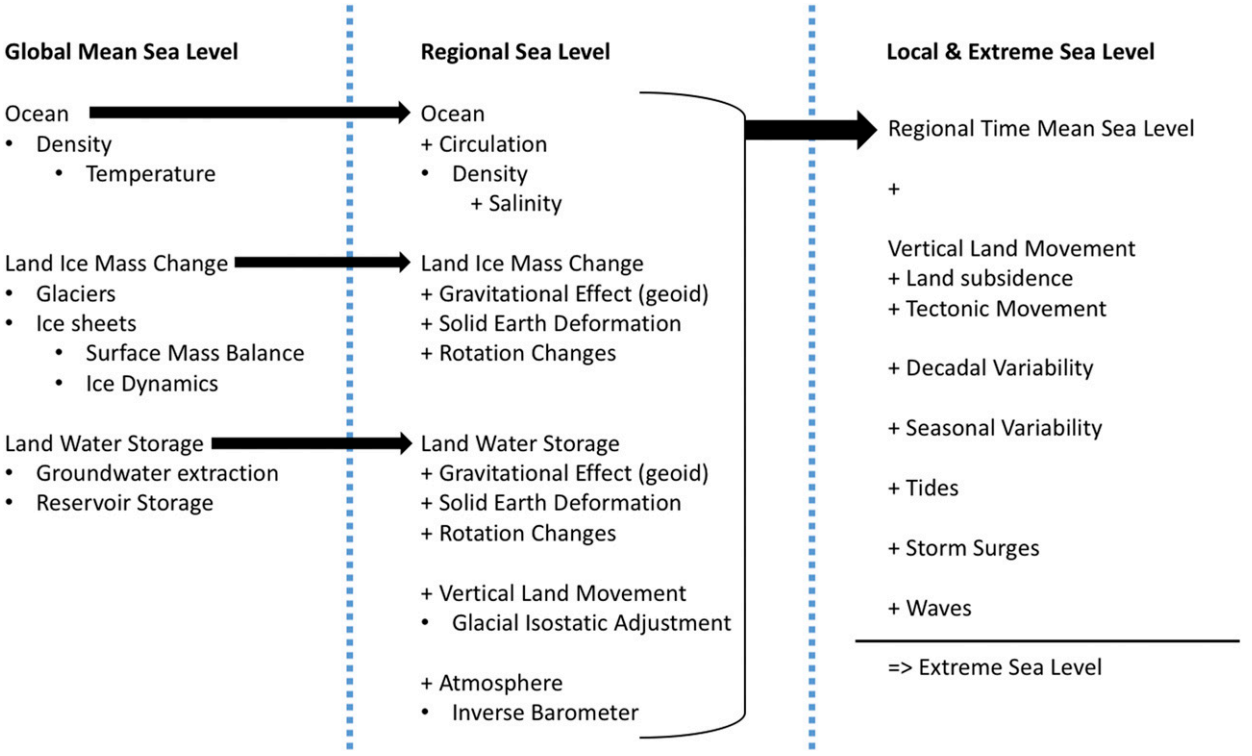

FIG. 1. The sea level "jigsaw": different processes (nonexhaustive) contributing to sea level change at a wide range of spatial and temporal scales.

changes. Ocean salinity changes, which also cause density variations, are negligible on a global scale (Lowe and Gregory 2006). Second, changes in land ice mass of glaciers and ice sheets (surface mass balance and ice dynamical processes) contribute to sea level change. In addition, changes in landwater storage due to human activity should be taken into account, most importantly reservoir building and groundwater extraction (Fig. 1, left). Natural changes in landwater storage, such as those resulting from snow cover, surface water, or soil moisture, are large on seasonal time scales and are found to be important up to decadal time scales (Reager et al. 2016) but are assumed to be small on century time scales (Wada et al. 2016; Church et al. 2013a).

This paper focuses on the global mean contributions to twentieth-century sea level change. However, it is important to note that sea level changes vary spatially, and additional processes come into play on smaller spatial and temporal scales (Fig. 1; e.g., Slangen et al. 2014a). At a regional scale this includes, for instance, changes in the ocean circulation (e.g., due to wind stress) or local ocean water density variations (both temperature and salinity driven). Other causes are changes in Earth's gravitational field and vertical land motion due to redistribution of mass between land and the ocean—both present-day ice mass change and glacial isostatic adjustment in response to ice mass loss after the Last Glacial Maximum (Spada 2017). See Part II of this paper by Meyssignac et al. (2017, hereafter M17) for a detailed discussion of these regional sea level change patterns. Even smaller scales are required when studying coastal sea level change and potential changes in sea level extremes (Fig. 1, right; e.g., Cannaby et al. 2016).

The main goal of this paper is to evaluate model simulations of the physical processes that contribute to global mean sea level (GMSL) change and to establish how well they can explain the observed GMSL change in the twentieth century. A comparison of the observed and simulated regional distribution of sea level change at individual tide gauge locations is presented in the accompanying paper (M17).

In recent decades, one of the major questions in sea level research has been the closure of the twentieth-century (global mean) sea level budget (Munk 2002; Church et al. 2011; Gregory et al. 2013a; Jevrejeva et al. 2017). There are several parts to this question: first, the sum of the observations for the individual components (Fig. 1, left) tends to underestimate the total observed change inferred from tide gauges, raising the issue of different types of uncertainties in the observations.

Second, the sum of model-based sea level contributions also tends to underestimate the total observed change for the twentieth century, probably because of uncertainties in both the models and the observations. Past observations of sea level change relying on tide gauges are spatially and temporally sparse, difficult to quality-control, and biased to the Northern Hemisphere. They may therefore not be fully representative of GMSL (Thompson et al. 2016) until satellite data started to become available in the early 1990s. The model-based contributions, on the other hand, may not fully account for all climate variability, such as multidecadal variations in the ocean, the delayed response of glaciers and ice sheets to externally driven climate change, and imperfections in the applied forcings and/or the model responses.

Recently, several large community efforts (Church et al. 2011; Gregory et al. 2013a) have explored a wide range of observational estimates of all contributions to sea level change, and were able to close the twentieth-century observational budget within uncertainties. In this paper, we focus on the second part of the problem, namely reconciling the simulated model estimates with observed GMSL change. This is an important topic, as a better understanding of and ability to model past sea level change increases confidence in the models' ability to project future sea level changes.

We build on and extend previous work that compared model estimates to observations of GMSL rise (e.g., Church et al. 2013b; Slangen et al. 2016). With respect to previous work, the time period has been extended to 2015, allowing for the longest possible time series of satellite observations to be included. The model estimates of the individual contributions to sea level rise have been updated and now use more recent information. For instance, the glacier model now uses a more recent and reliable version of the Randolph Glacier Inventory than in Church et al. (2013b) and the estimate of groundwater extraction is updated following recent publications (Döll et al. 2014; Wada et al. 2016).

We present a consistent model dataset that uses the same set of climate models to estimate the glacier contribution, the surface mass balance of the Greenland and Antarctic ice sheets, and the ocean thermal expansion. This is a different approach from that in the work of Church et al. (2013b), where thermal expansion and the glacier contribution were simulated with different climate model ensembles. In addition, we provide separate estimates for contributions of surface mass balance (based on CMIP5 climate model output) and ice dynamics of the Greenland and Antarctic ice sheets, which in Church et al. (2013b) were estimated with a constant of $0.1\,\mathrm{mm\,yr^{-1}}$. Here, the use of a consistent set of models for an increased number of contributions allows us to evaluate the individual model simulations rather than the model ensemble alone.

The simulated sea level changes are completed by extended observation-based estimates of ice sheet dynamical processes and landwater storage changes. These estimates are compared to tide gauge reconstructions for the period 1900–2007 and to satellite altimetry for the period 1993–2015. This allows us to quantify and study the acceleration in sea level rise from the early 1990s onward.

We also discuss potential additional contributions that should be included in the comparison between model-based estimates and observations. These contributions are all based on observational evidence and are currently absent or poorly represented in climate models. In addition, observational estimates are particularly sparse due to limited accessibility and the large surface area of the ice sheets. While it has been generally assumed that the historical contributions of the ice sheets are small compared to thermal expansion and glacier mass change, a recent study suggests a more substantial contribution of $25 \pm 9\,\mathrm{mm}$ (1σ) from the Greenland ice sheet over the twentieth century arising from internal climate variability and/or the response to increased radiative forcing (Kjeldsen et al. 2015).

We first present the observational estimates of GMSL and the climate models and experiments that we use in our comparisons (section 2). The individual contributions to GMSL change, both simulated and observed, are discussed in section 3. In section 4 we combine the model-simulated estimates and compare them to tide gauge reconstructions (1900–2007) and satellite measurements (1993–2015).

2. Data

a. *Sea level observations*

For most of the twentieth century, tide gauges are the only source providing sea level measurements. This is not ideal, as tide gauges (particularly the ones going further back in time) are distributed unevenly around the world and are confined to coastal locations. It is therefore not correct to take a simple average, as this would result in a biased global mean sea level record (Thompson et al. 2016). Instead, several methods have been developed to reconstruct the sea level field and obtain an estimate of GMSL change back to 1900 using tide gauges. Here we use four different reconstructions. The first one is from Church and White (2011), an update of their previous work (Church and White 2006) in which they reconstructed historical sea levels by deriving empirical orthogonal functions (EOFs) from satellite data and used the EOFs to find the best fit to

the tide gauge records. These data were downloaded from www.cmar.csiro.au/sealevel/ and provide yearly values from 1880 to 2013. Ray and Douglas (2011) provide the second reconstruction time series (downloaded from www.psmsl.org) with yearly values for 1900–2007. They use a method similar to that of Church et al. but with differences in details of the methodology. With respect to Church et al. (2013b) we add two more recent tide gauge reconstructions, constructed using different methods. The reconstruction from Jevrejeva et al. (2014) (downloaded from www.psmsl.org) provides monthly values for 1807–2010. This reconstruction uses the ''virtual station'' method, where 1277 tide gauge records are divided into 14 regions to overcome a geographical bias in the data, and these regions are then averaged to obtain the global mean change. Finally, the reconstruction from Hay et al. (2015) (downloaded from http://www.nature.com/nature/journal/v517/n7535/source_data/nature14093-f2.xls; their Fig. 2 source data) provides yearly values for 1900–2010. These authors have used Kalman smoothing to process the spatially and temporally sparse tide gauge data and combine this with spatial fingerprints from the different sea level contributions.

Since 1993, satellite altimetry has provided more globally complete observations of sea level change (covering at least 66°S–66°N and up to 82°N/S for *Envisat*). Here we use three different global mean time series, which all include measurements from the consecutive TOPEX/Poseidon, *Jason-1*, and *Jason-2* satellite missions, but with different choices in instrumental and geophysical corrections and in the algorithms used to compute the GMSL time series (Masters et al. 2012; Henry et al. 2014). We use a time series from the European Space Agency (ESA) sea level climate change initiative (CCI) (Ablain et al. 2015; http://www.esa-sealevel-cci.org), which in addition includes data from the *ERS-1* and *-2* and *Envisat* satellite missions. The data have been corrected for the seasonal signal (annual and semiannual), inverse barometer (IB), and glacial isostatic adjustment (GIA; $-0.3\,\mathrm{mm\,yr^{-1}}$; Tamisiea 2011). The second time series, from CSIRO (Church and White 2011; www.cmar.csiro.au/sealevel/), is also corrected for the seasonal signal, IB, and GIA. The third time series is from Watson et al. (2015), who suggested a bias correction for an inferred drift in the early part of the altimeter record, based on the difference between the CSIRO time series and tide gauge observations (where the tide gauges were corrected for vertical land movement using GPS data), which mainly influences the TOPEX part of the satellite record. This bias correction is a different approach than in the other two satellite time series (CSIRO and ESA-CCI), both of which are completely independent from tide gauge measurements.

b. Model data

To model the twentieth-century contributions to sea level change, we mainly use data from phase 5 of the Climate Model Intercomparison Project (CMIP5; Taylor et al. 2012). These data are used to evaluate ocean thermal expansion and to compute the contributions from glaciers and ice sheet surface mass balance using offline models. To cover the period 1900–2015 (as all four reconstructions provide data from 1900 onward), the historical model simulations (1850–2005) were extended using the representative concentration pathway (RCP) projections from the CMIP5 database (Moss et al. 2010), where we used the RCP8.5 scenario out of the four scenarios available (RCP2.6, 4.5, 6.0, and 8.5). This RCP projects a radiative forcing increase of $>8.5\,\mathrm{W\,m^{-2}}$ in 2100 relative to preindustrial conditions. The choice for the RCP8.5 scenario was based on availability, as most models are available for RCP4.5 and 8.5, and less for RCP2.6 and 6.0. However, this is not critical to our results, as the different scenarios only start to diverge significantly after the year 2030 (Church et al. 2013a).

The following CMIP5 variables were used: ''zostoga'' (global mean ocean thermal expansion), ''to'' (ocean temperature), ''so'' (ocean salinity), ''tas'' and ''ta'' (air temperature at surface and at 600 hPa, respectively), ''pr'' (precipitation), ''prsn'' (snowfall), and ''evspsbl'' (evaporation). The ocean variables (zostoga, tos, so) were dedrifted by computing linear fits on the full control run (which is forced by nonevolving preindustrial conditions) and then subtracting the time-corresponding part of the fit of each models' preindustrial control simulation from the historical simulation. The use of a linear fit ensures that the drift is removed but no physical trends are, which is particularly relevant for the regional change in the companion paper (M17). In addition, Hobbs et al. (2016) showed that the use of a linear fit is an adequate dedrifting method particularly for global quantities, and there is no additional gain from using higher-order fits. Dedrifting of ocean variables is necessary to account for spurious trends that result from the (deep) ocean not being in equilibrium with the forcing conditions (e.g., Sen Gupta et al. 2013) and/or to correct for imperfect representation of the global energy budget (Hobbs et al. 2016). We present annual time series unless stated otherwise. Details on how the CMIP5 variables were used to compute each of the sea level contributions will be discussed in section 3.

To obtain a consistent set of models for all contributions, the selection of atmosphere–ocean general circulation models (AOGCMs; Table 1) is based on the availability of all of the abovementioned required variables, resulting

TABLE 1. CMIP5 climate models used in this study, indicating the presence or absence of volcanic forcing in the preindustrial control simulation (data accessed 2015/16). (Expansions of acronyms are available online at http://www.ametsoc.org/PubsAcronymList.)

Model ID	Volcanic forcing in preindustrial control run?	Institute, country (reference)
CanESM2	No	Canadian Centre for Climate Modelling and Analysis, Canada (Yang and Saenko 2012)
CCSM4	No	National Center for Atmospheric Research, United States (Gent et al. 2011)
CNRM-CM5	Yes	Météo-France/Centre National de Recherches Météorologiques, France (Voldoire et al. 2013)
GFDL-CM3	No	National Oceanic and Atmospheric Administration/Geophysical Fluid Dynamics Laboratory, United States (Griffies et al. 2011)
GISS-E2-R	Yes	National Aeronautics and Space Administration Goddard Institute for Space Studies, United States (Schmidt et al. 2014)
HadGEM2-ES	Yes	Met Office Hadley Centre, United Kingdom (Martin et al. 2011)
IPSL-CM5A-LR	Yes	Institut Pierre-Simon Laplace, France (Dufresne et al. 2013)
MIROC5	Yes	The University of Tokyo, Japan (Watanabe et al. 2010)
MIROC-ESM	Yes	The University of Tokyo, Japan (Watanabe et al. 2011)
MPI-ESM-LR	No	Max Planck Institute for Meteorology, Germany (Giorgetta et al. 2013)
MRI-CGCM3	No	Meteorological Research Institute, Japan (Yukimoto et al. 2012)
NorESM1-M	Yes	Norwegian Climate Centre, Norway (Bentsen et al. 2013)

in a set of 12 models. From each model, the first available realization (r1i1p1) was used. Comparisons for the thermal expansion contribution show that this set of models and realizations is representative of the larger CMIP5 ensemble as used in Slangen et al. (2014a, 2015). The same set of 12 models is used in the M17 companion paper, which focuses on regional sea level patterns rather than the global mean.

3. Contributions to twentieth-century global mean sea level change

In this section, we discuss the processes that influence GMSL change. We will explain how each contribution is evaluated, and compare the simulated contributions to observations where available.

a. Thermal expansion

Thermal expansion is one of the major contributors to twentieth-century GMSL (Church et al. 2013a) and is the only contribution that is simulated directly in the CMIP5 models. Averaged over the global oceans the density change due to salinity variations largely cancels out, and steric GMSL change is driven by temperature variations alone (Lowe and Gregory 2006).

We use two different ways to estimate model-based thermal expansion. The first uses the CMIP5 variable zostoga as it is provided by the CMIP5 modeling groups, which represents the thermal expansion over the entire model ocean basin and full depth of the ocean. However, most of the observational estimates of thermal expansion are only provided for the top 700 m of the ocean. Therefore, we also use a thermal expansion estimate derived from annual three-dimensional model fields of ocean potential temperature (to) in combination with a salinity (so) climatology, using the 1980 United Nations Educational, Scientific and Cultural Organization (UNESCO) international equation of state (IES80), following Melet and Meyssignac (2015). We use each models' native grid for the computation, for two different depths: 0–700 m (TS_{700}) and full depth (TS_{full}). Semienclosed basins (e.g., the Mediterranean Sea, Black Sea, Red Sea, Caspian Sea, Baltic Sea, Hudson Bay, and Great Lakes) are excluded from the TS computation, as ocean temperatures in some of the CMIP5 models are less reliable in these regions (Melet and Meyssignac 2015).

Five of the 12 climate models have no volcanic forcing included in their preindustrial control run (Table 1). As a result of the absence of volcanic forcing in the control run, the introduction of volcanic forcing in the historical simulations results in a cooling of the ocean, which leads to an underestimate of the thermal expansion for the twentieth century (Gregory 2010; Gregory et al. 2013b). This effect is visible in historical natural-only simulations (Slangen et al. 2015), which are not expected to show a long-term thermal expansion trend. To estimate the magnitude of the response to the introduction of volcanic forcing, we derive the global mean trend over 1850–2005 of the historical natural-only forced simulations for these models where possible (three models for zostoga and four for TS; Table 2), and otherwise use a constant value of 0.1 mm yr^{-1} as suggested in Gregory et al. (2013b) (two models for zostoga and one for TS). The derived values (Table 2) are then used to correct the historical simulations. This is a

TABLE 2. Linear correction factors (mm yr^{-1}) for runs without preindustrial volcanic forcing. Factors are derived from historical natural-only forced simulations where possible, or using the Gregory et al. (2013b) estimate of 0.1 mm yr^{-1} as a constant value otherwise (denoted as cst). Note: A smaller correction to account for the reduced depth in TS_{700} MPI-ESM-LR has been tested (as low as 0.05 mm yr^{-1}) but was found not to change the ensemble mean and standard deviation, so for simplicity we use 0.10 mm yr^{-1} also as a 0–700-m constant.

	Zostoga (full depth)	TS_{full}	TS_{700}
CanESM2	0.10	0.13	0.06
CCSM4	0.10 (cst)	0.09	0.05
GFDL-CM3	0.19	0.16	0.10
MPI-ESM-LR	0.10 (cst)	0.10 (cst)	0.10 (cst)
MRI-CGCM3	0.00	0.05	0.03

refinement in the methodology compared to Church et al. (2013b), where a correction of 0.1 mm yr^{-1} was added to all the model results.

The model results are compared to three observational reconstructions of thermosteric change. These reconstructions are all derived from in situ temperature measurements in the ocean, with the largest coverage and smallest uncertainties at the present day, and sparser data with larger uncertainties going back in time. For the upper 700 m of the ocean, we use annual time series from the three different reconstructions, which all use ocean temperature profiles as input, but the data are selected and processed in different ways to arrive at a global mean estimate:

1) Domingues et al. (2008), updated to version 3.1 (1950–2012),
2) Ishii and Kimoto (2009), updated to version 6.14 (1945–2014), and
3) National Oceanographic Data Center (NODC; Levitus et al. 2012, 1957–2013).

Variations among the reconstructions can arise due to differences in the 1) input data and quality control procedures, 2) application and approach to correct interplatform biases, 3) choice of reference climatology, and 4) choice of mapping methods (Palmer et al. 2010; Abraham et al. 2013; Boyer et al. 2016).

To estimate the full depth thermal expansion, we use the 0–2000-m time series of NODC to compute the 700–2000-m contribution (1957–2013) and add a constant of 0.18 mm yr^{-1} for that same period, based on Purkey et al. (2014), to account for change in the deep ocean below 2000 m. All time series were downloaded on 9 June 2016. The common time period between the different observational time series is 1957–2012 (Table 3).

For the full depth of the ocean, the differences between TS_{full} and zostoga are small for most models (Fig. 2a). Note that TS_{full} (corrected) has an ensemble mean change from 1901–20 to 1996–2015 of 46 ± 33 mm (the uncertainty indicating the 1.65σ CMIP5 model spread), which is 3 mm larger than the zostoga ensemble mean, and each volcanically corrected ensemble is 4 mm larger than the respective uncorrected ensemble (Table 3). While the uncorrected CMIP5 ensemble mean is at the lower end of the observational range (Table 3), the corrected ensemble mean provides quite a good fit to the observations of Domingues et al. (2008) and NODC, although the difference is probably not significant given the uncertainty ranges of both models and observations. However, the spread in the models is larger than the observational uncertainties, which is consistent with studies where the observed ocean heat content was compared to climate model simulations (Cheng et al. 2016; Gleckler et al. 2016).

TABLE 3. Summary of different options for the modeled thermal expansion contribution to sea level change from 1901–20 to 1996–2015 and from 1957–61 to 2008–12 (mm ± 1.65σ), and the available observational estimates for the later period only for full depth and 0–700 m. The uncertainties in the model estimates are determined by the CMIP5 model spread; the observational uncertainties were provided with the observational time series.

			Thermal expansion contribution (mm)	
Variable	Depth	Volcanic correction	From 1901–20 to 1996–2015	From 1957–61 to 2008–12
Zostoga	Full	No	40 ± 30	31 ± 23
Zostoga	Full	Yes	43 ± 30	33 ± 23
TS_{full}	Full	No	43 ± 32	33 ± 25
TS_{full}	Full	Yes	47 ± 32	36 ± 25
Obs-Domingues	Full	—	—	38 ± 15
Obs-Ishii	Full	—	—	33 ± 7
Obs-NODC	Full	—	—	40 ± 8
TS_{700}	0–700 m	No	28 ± 22	22 ± 17
TS_{700}	0–700 m	Yes	31 ± 23	23 ± 18
Obs-Domingues	0–700 m	—	—	19 ± 15
Obs-Ishii	0–700 m	—	—	15 ± 5
Obs-NODC	0–700 m	—	—	21 ± 5

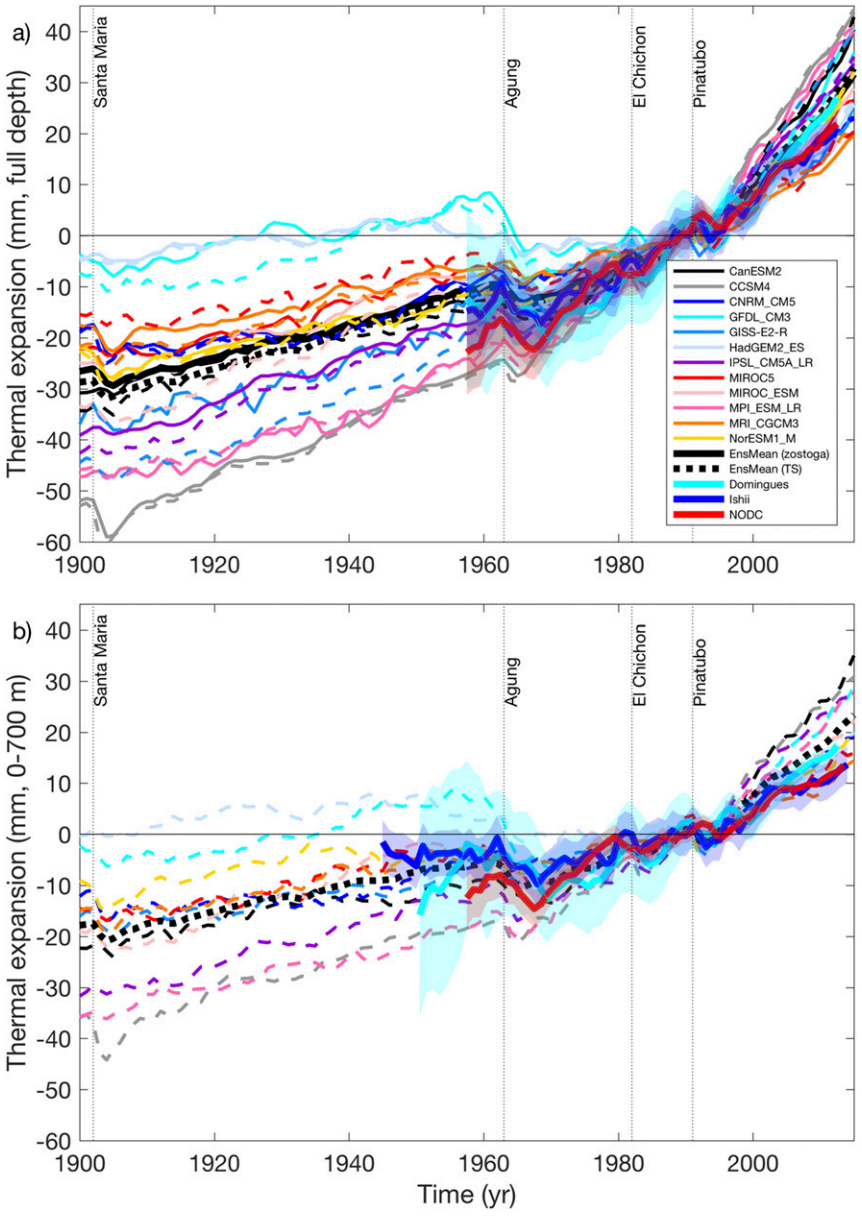

FIG. 2. Modeled thermal expansion contribution to sea level change (1900–2015; mm) for (a) full depth, zostoga (solid) and TS_{full} (dashed), and (b) 0–700 m, TS_{700} only (dashed); ensemble mean in thick black, relative to a baseline period of 1980–2000. Corrected for volcanic absence in the preindustrial control using the linear trend in the historical-natural only simulation (Table 2). Compared to observations (shading indicates 1.65σ; Domingues in cyan, Ishii in blue, and NODC in red), in (a) all three observational time series include the 700–2000-m NODC and >2000 m Purkey et al. (2014) contributions. Major volcanic eruptions indicated with dashed vertical lines.

There are some individual models where the differences are larger between zostoga and TS_{full}, such as GFDL-CM3, MIROC5, MIROC-ESM, and GISS-E2-R. The main reason for this is probably the difference in land–ocean mask (i.e., inclusion/exclusion of marginal seas): some of these models have no connection between marginal seas and the open ocean, causing overestimated thermal expansion in the marginal seas (Melet and Meyssignac 2015).

Focusing on the upper 700 m of the ocean, the volcanic corrected TS_{700} model ensemble mean change (Fig. 2b, Table 3) agrees best with the total change in the NODC observational time series (21 ± 5 mm from 1957–61 to

2008–12), while the Ishii observational time series shows a smaller change (15 ± 5 mm) which is reproduced by some members of the climate model ensemble. When comparing observations to climate models, it is important to note that while historical external radiative forcing is used to drive the climate models, the models are not expected to match the historical internal climate variability (this includes, for instance, the timing of El Niños). This explains part of the discrepancies in the temporal variability of the observations compared to the models on annual to decadal time scales. However, there are also some consistent features. The response to volcanic forcing is present in the simulated thermal expansion (as this is part of the prescribed external forcing) and also in all three observation time series. For instance, there is a decrease between 1963 and 1970 that can be attributed to the Mount Agung volcanic eruption in 1963, and similar responses occur after the El Chichón and Mount Pinatubo eruptions (Fig. 2). The response between the models and volcanic eruptions varies because of different model responses to aerosol forcing (Slangen et al. 2015) and also because some volcanic forcing was longer sustained than others (e.g., Mount Agung; von Schuckmann et al. 2016). Note that, because of observational uncertainties, the statistical significance of the observed response is limited by the quality and coverage of the available pre-Argo observations (Cheng et al. 2017).

b. *Glaciers*

The mass loss of glaciers and ice caps around the world represents another major contribution to GMSL (Church et al. 2013a; Marzeion et al. 2017). The glacier contribution is simulated with a global glacier mass balance model (Marzeion et al. 2012, 2015). The model is driven by CMIP5 temperature (tas) and precipitation (pr), using the same CMIP5 models and simulations as for the thermal expansion contribution. The present-day glacier area used in the model is the Randolph Glacier Inventory, version 4.0 (Arendt et al. 2014), which is the state-of-the-art global glacier inventory. Mainly as a result of the updated glacier inventory and improvements in the digital elevation model (Marzeion et al. 2015; Slangen et al. 2017), these new glacier model results find a reduced glacier contribution compared to the results presented in Marzeion et al. (2012) and Church et al. (2013b). Antarctic peripheral glaciers are excluded from the model (see section 5). The glacier model first iteratively determines each glacier's area and vertical extent in 1900, and is then forced by CMIP5 data to model the glacier evolution over the twentieth century and the resulting contributions to GMSL.

We use three different observation-based estimates of the global glacier mass contribution to GMSL. The first estimate is derived from glacier length records (Leclercq et al. 2011), which were updated with additional length records in Greenland and extended to 2010 as described in Marzeion et al. (2015). The second estimate is based on geodetic and direct mass change observations (Cogley 2009), using release 1301 as in Marzeion et al. (2015). Third, we use a modeled mass change estimate from the updated global glacier mass balance model of Marzeion et al. (2012, 2015) driven by gridded climate observations [Climatic Research Unit Time Series (CRU TS 3.22); Harris et al. 2014]. As this is based on observed temperature and precipitation data, the resulting modeled glacier mass balance changes follow the historical climate variability.

The CMIP5 ensemble mean contribution of the glaciers over the twentieth century (from 1901–20 to 1996–2015) is 55 ± 13 mm (Fig. 3; 1.65σ uncertainty based on CMIP5 model spread). The observational estimate by Leclercq et al. (2011) for 1900–2010 (86 ± 36 mm, gray shading) is larger than the modeled estimate for that same period (64 ± 17 mm for 1900–2010). The glacier-model estimate forced by temperature and precipitation from the CRU gridded data is only slightly larger for 1900–2010 (67 ± 13 mm; red solid line in Fig. 3) but larger than any of the individual models for the first half of the twentieth century. The differences are reduced in the second half of the twentieth century, when the Cogley (2009) observations are also available. The Cogley (2009) data suggest a contribution of 42 mm for 1950–2015 (blue shading, uncertainty estimated at 10% of the total value), compared to 42 ± 10 mm for the CMIP5 ensemble for that same period (uncertainty based on the CMIP5 ensemble spread).

In the beginning of the twentieth century, both the Leclercq et al. (2011) observations and the CRU-driven model results show a different behavior than the CMIP5-driven model results (Fig. 3). Despite larger uncertainties in earlier observational estimates, the combination of glacier observations and CRU-driven model results suggests that there is some common variability in the observations (both in the glacier length records from Leclercq and in the CRU data) that is not reproduced in the CMIP5 models. A closer look at the regions (Marzeion et al. 2012) shows that most of the difference in the global mean is caused by a discrepancy in mass change in the glaciated regions around Greenland, corresponding to a period of warming and strong glacier melt that is present in the CRU-forced model and also found in observations (Bjørk et al. 2012), but not replicated by the CMIP5 models. There may be several reasons for this. As was mentioned before, the climate models are not forced to follow the "real world" internal climate variability; they are only forced by

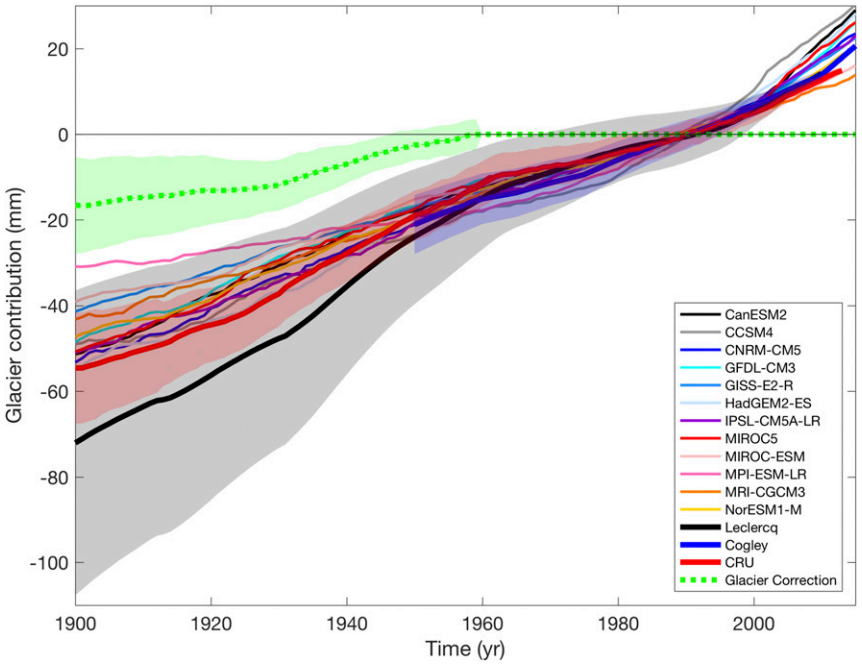

FIG. 3. Modeled glacier contribution to sea level change (1900–2015; mm; solid lines, excluding Antarctic PG), relative to a baseline period of 1980–2000, compared to observations [Leclercq et al. (2011) in black, Cogley (2009) in blue, and CRU-driven model in red; shading indicates 1.65σ]. Green dashes and shading indicate the proposed bias correction based on the mean difference of Leclercq et al. (2011) and CRU-driven model vs the CMIP5-driven estimates.

changes in external radiative forcing (e.g., through changing greenhouse gas concentrations and aerosol concentrations). Another reason may be a bias that was found in the atmospheric circulation of the climate models, which do not reproduce warm airflow over the south of Greenland, resulting in too little melt in this region (Fettweis et al. 2013). Third, the spatial patterns of the historical (natural and anthropogenic) aerosol forcing that drive the CMIP5 models are more uncertain going back in time (which may cause discrepancies in regional response of the model), and the (regional) response of climate models to aerosols in general is relatively uncertain compared to the response to greenhouse gas forcing. We therefore propose a bias correction to account for the reduced response in the climate models. We follow the approach of Slangen et al. (2016), and compute the ensemble mean difference between the CMIP5 models and the observation-based estimates [averaging the available twentieth-century Leclercq et al. (2011) and CRU-based observational estimates] to account for additional mass change in glaciers around Greenland in the early twentieth century. The proposed correction amounts to 15 ± 10 mm over the period from 1901–20 to 1996–2015 (Fig. 3, green dashed line; 1.65σ uncertainty from CMIP5 model spread). This correction is consistent with a 20-mm correction proposed in Church et al. (2013b) to account for internal variability in Greenland temperatures, and both corrections have the largest rates between 1930 and 1960. As the difference is very small after 1960, the correction is set to zero for the period 1960–2015.

c. *Ice sheets*

1) SURFACE MASS BALANCE

(i) Greenland surface mass balance

The modeled Greenland surface mass balance (SMB) contribution to twentieth-century GMSL is estimated using a regional statistical downscaling technique, which accounts for the nonuniform distribution of SMB change over Greenland (M17). Quadratic relations between the Greenland SMB change and CMIP5 variables (annual snowfall, CMIP5 variable prsn, and atmospheric summer temperature at 600 hPa, CMIP5 variable ta) were derived using CMIP5-forced MARv3.5 regional climate model simulations (Fettweis et al. 2013). MARv3.5 has only been forced with three CMIP5 models (MIROC5, NorESM1-M, and CanESM2) over 1900–2006 due to computational limitations. The inferred statistical downscaling is then applied to the other climate model output.

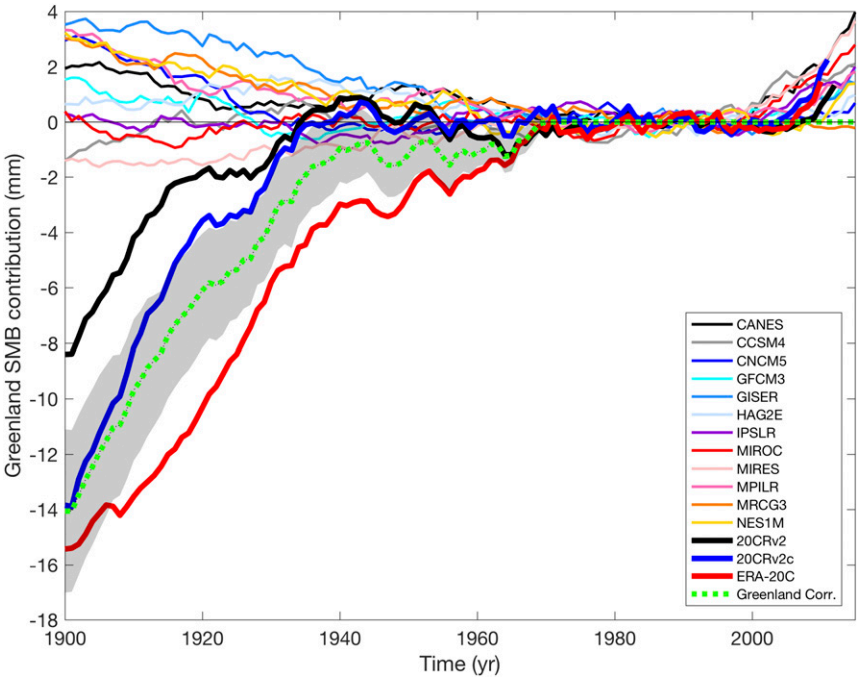

FIG. 4. Modeled Greenland SMB contribution to sea level change (1900–2015; mm; solid lines), using CMIP5 results, relative to a baseline period of 1980–2000, compared to reanalysis-driven estimates (thick solid lines; 20CRv2 in black, 20CRv2c in blue, and ERA-20C in red). Proposed correction for early-twentieth-century variability (mean of the three reanalyses minus mean of CMIP5 models) shown in stippled green line and gray shading ($\pm 1.65\sigma$).

This downscaling technique uses six major drainage basins of the Greenland ice sheet.

There are no direct observational time series of Greenland SMB in the twentieth century, but an observational estimate can be obtained using reanalysis data (instead of CMIP5 data) and the downscaling relation between temperature, precipitation, and SMB (Fettweis et al. 2013). Three reanalysis products are used to provide the observation-based estimate: ERA-20C (Poli et al. 2016), 20CRv2, and 20CRv2c (Compo et al. 2011).

The CMIP5-derived Greenland SMB contribution is at least an order of magnitude smaller than the contributions from glaciers and thermal expansion (Fig. 4). The ensemble mean contribution amounts to 0 ± 3 mm (1.65σ CMIP5 model spread) over the period 1901–20 to 1996–2015. For the period since 1990, both the CMIP5 results and the reanalyses show a sharp increase in the Greenland SMB contribution to GMSL, which is confirmed by observations and regional climate modeling (van Angelen et al. 2014). In the beginning of the twentieth century, the three reanalysis-based Greenland SMB estimates lead to a significantly larger contribution to GMSL than the CMIP5 models (Fig. 4), similar to the glacier contribution (section 3b). This is thought to be caused by an increase in air temperatures in and around Greenland around 1900–40, which led to increased melt in Greenland (Box et al. 2009; Bjørk et al. 2012; Fettweis et al. 2017) and surrounding glaciers (section 3b; Marzeion et al. 2012). This temperature increase is found in the reanalyses but not in the CMIP5 models. Similar to the approach for the glaciers, we propose a bias correction to account for this additional internal climate variability using the difference between the mean of the observational estimates and the CMIP5 ensemble mean (Fig. 4, dotted green line), which is 10 ± 4 mm from 1901–20 to 1996–2015 (1.65σ CMIP5 model spread) and set to zero from 1970 onward. Although this correction seems substantial, the corrected Greenland SMB contribution is a low-end estimate compared to independent observational evidence (Kjeldsen et al. 2015), suggesting a contribution of the whole of the Greenland ice sheet of 25 ± 9 mm (1σ) over the twentieth century. Note that the Kjeldsen estimate includes both SMB and ice dynamical changes but excludes glaciers peripheral to the Greenland ice sheet.

(ii) Antarctic surface mass balance

The contribution of Antarctic SMB changes to twentieth-century GMSL is estimated with two different methods, both using CMIP5 data. The first method uses the difference between precipitation (CMIP5 variable pr) and evaporation (CMIP5 variable evspsbl) on the

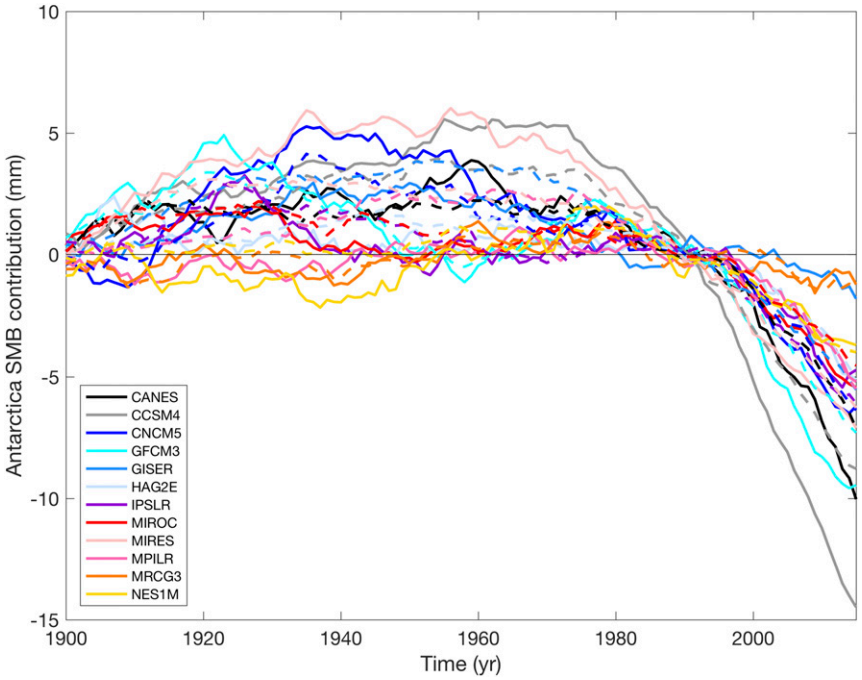

FIG. 5. Modeled Antarctic surface mass balance contribution to sea level change (1900–2015; mm), relative to a baseline period of 1980–2000, estimated using PME (solid) and temperature–precipitation relation (TAS; dashed lines).

Antarctic ice sheet [precipitation minus evaporation (PME)]. Although CMIP5 models usually have no correct representation of snowpack processes, the freshwater runoff on the Antarctic ice sheet is negligible for the twentieth century (Lenaerts et al. 2012), and thus PME is sufficient to represent the Antarctic SMB. The resulting SMB time series are scaled to fit the best estimate of the Antarctic SMB for the period 1985–2010 (merging historical and RCP8.5 experiments to go beyond 2005) from the regional climate model RACMO2.1 forced by ERA-Interim data (Lenaerts et al. 2012).

The second method to estimate Antarctic SMB changes uses CMIP5 surface temperature changes to estimate the change in precipitation over the Antarctic ice sheet (henceforth TAS), again with respect to the best estimate SMB from Lenaerts et al. (2012). As warmer air has a higher moisture holding capacity, the snowfall over Antarctica increases when temperatures increase, thus impacting the SMB of the ice sheet. The change in SMB is estimated at approximately 6% ± 0.7% K^{-1}, which is consistent with observations (ice cores) and different global and regional climate models (Ligtenberg et al. 2013; Frieler et al. 2015).

The modeled SMB ensemble mean estimates from both methods show a small sea level fall over the twentieth century of −6 ± 3 mm for the TAS method and −6 ± 7 mm for the PME method (Fig. 5; 1.65σ model spread). The spread in the PME estimates is larger than in the TAS estimates (i.e., solid lines in Fig. 5 compared to dashed lines), probably because temperature is a more robust variable in the models than precipitation and evaporation. However, in the ensemble mean there is no significant difference for the 1900–2015 period. Both methods initially show only a minor Antarctic SMB contribution to GMSL (only 1 ± 3 mm up to 1970) but indicate an accelerated sea level fall from 1970 onward (−7 ± 5 mm for TAS and −8 ± 8 mm for PME between 1971 and 2015).

However, we note that although the relation between increasing temperature and increasing precipitation is robust, this small sea level fall is not yet significant when considering the large internal (snowfall) variability in Antarctic SMB change (on the order of 0.3–0.4 mm yr^{-1}). A recent publication estimated that the signal is only projected to emerge from the noise in the first half of the twenty-first century (Previdi et al. 2016). This is in line with regional climate model results, which found no significant trend in Antarctic SMB for the period 1979–2010 (Lenaerts et al. 2012).

2) ICE SHEET DYNAMICS

Apart from changes in the surface mass balance, the Greenland and Antarctic ice sheets can also contribute to GMSL due to changes in dynamical discharge processes. Processes that could contribute to dynamical

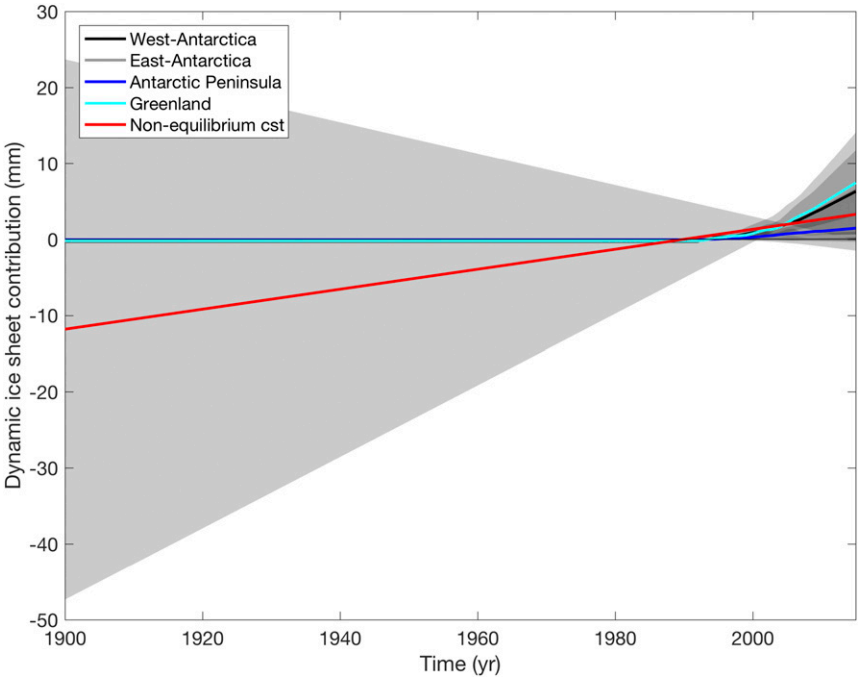

FIG. 6. Dynamic discharge contributions of the ice sheets to sea level change (1900–2015; mm; $\pm 1.65\sigma$), relative to a baseline period of 1980–2000. The Antarctic and Greenland estimates are based on Shepherd et al. (2012) and extended using recent data (see text for references). The proposed nonequilibrium constant is taken from Slangen et al. (2016) and represents an ongoing contribution from the ice sheets and deep ocean as a result of nonequilibrium due to long response times.

discharge include, for instance, the melt of floating ice shelves due to ocean warming or calving of marine-terminating glaciers (Church et al. 2013a, and references therein). However, these processes are not included in CMIP5 models and therefore have to be estimated in another way.

Here we use the time series from Shepherd et al. (2012), a community effort to present a complete ice sheet mass balance estimate that reconciled different methods and models. The total ice sheet mass balance estimate is available from 1993 to 2010 in four regions: West Antarctica, East Antarctica, the Antarctic Peninsula, and Greenland. The ice-dynamical estimate is computed by removing the SMB (based on RACMO2.1; Lenaerts et al. 2012; van Angelen et al. 2014) from the total ice sheet mass balance estimate. The ice dynamical time series are extended to 2015 using discharge estimates from Sutterley et al. (2014) and Enderlin et al. (2014), which assume that the West Antarctic discharge was slightly above the 2008–12 average and that the Greenland ice sheet discharge remained constant at the 2010 value. Discharge for East Antarctica and the Antarctic Peninsula is assumed to follow the 2001–10 average. The extrapolated values are in line with recent ice sheet mass balance studies (Velicogna et al. 2014; Harig and Simons 2015; McMillan et al. 2016).

The resulting total ice-dynamical contribution to GMSL over the period from 1993–95 to 2011–15 is 7 ± 4 mm from the Greenland ice sheet and 7 ± 8 mm from the Antarctic ice sheet (Fig. 6, Table 4). The 1σ uncertainties on the ice dynamics are derived by assuming they have the same uncertainty-to-signal ratios as the total mass balance change presented in Table 1 of Shepherd et al. (2012), which is 35% for Greenland and 75% for Antarctica.

Several studies have suggested that in the twentieth century there was a nonzero contribution to GMSL from long-term nonequilibrium changes on the ice sheets and/or in the deep ocean as a result of their relatively long response times to climate variations, which is not represented in the models (e.g., Gregory et al. 2013b; Church et al. 2011, 2013b). In Gregory et al. (2013a), this long-term change was suggested to range between 0 and 0.4 mm yr^{-1}, the majority from Antarctica, which is supported by Masson-Delmotte et al. (2013), who find geological evidence for an ongoing long-term GMSL contribution of about 0.2 mm yr^{-1} in the last two millennia. This long-term change is not represented in the modeled SMB

TABLE 4. Modeled sea level contributions from 1901–20 to 1996–2015 and from 1993–97 to 2011–15 (mm ± 1.65σ). Uncertainties are assumed to be independent and computed by taking the square root of the sum of the individual contributions' squared uncertainties. Footnotes provide definitions of uncertainties.

Contribution	Description	Sea level contribution (mm)	
		1901–20 to 1996–2015	1993–97 to 2011–15
Thermal expansion	Zostoga—volcanic correction[a]	43 ± 30	26 ± 12
	TS_{full}—volcanic correction[a]	47 ± 32	27 ± 11
	Total thermal expansion[b]	45 ± 44	27 ± 16
Glaciers	Glaciers[a]	55 ± 13	18 ± 7
	Early 20thC correction[a]	15 ± 10	—
	Total glaciers[b] (excluding correction)	55 ± 13	18 ± 7 mm
	Total glaciers[b] (including correction)	70 ± 16	18 ± 7
Ice sheets	Greenland SMB[a]	0 ± 3	1 ± 2
	GrSMB early 20thC correction[a]	10 ± 4	—
	Antarctica SMB[c]	−4 ± 6	−5 ± 6
	Greenland dynamics[d]	3 ± 2	7 ± 4
	Antarctica dynamics[d]	4 ± 5	7 ± 8
	Non-equilibrium constant[e]	12 ± 32	2 ± 6
	Total ice sheets[b] (excluding correction)	3 ± 9	9 ± 11
	Total ice sheets[b] (including correction)	25 ± 33	12 ± 12
Landwater	Reservoir storage[f]	−25	−4
	Groundwater—Wada16[f]	16	6
	Groundwater—Döll[f]	11	5
	Total landwater[g]	−11 ± 7	2 ± 2
Total	Models[h] (excluding correction)	92 ± 47	56 ± 18
	Models[h] (including correction)	129 ± 58	58 ± 19

[a] Based on CMIP5 model spread.
[b] Square root of the squared sum of uncertainties in this category.
[c] Square root of the squared sum of the CMIP5-based TAS and PME uncertainties.
[d] Based on Shepherd et al. (2012, their Table 1) the 1σ uncertainties are estimated at 35% (GIS) and 75% (AIS).
[e] Based on Slangen et al. (2016, their Fig. S2) the uncertainty is estimated at 0.21 mm yr^{-1}.
[f] No uncertainties provided in source data.
[g] Uncertainty taken as the difference between the two groundwater estimates.
[h] Square root of the squared sum of uncertainties.

changes, which assumes a much faster response to climate changes. It is also important to keep in mind that in the climate models the dedrifting procedure removes long-term trends, which imposes an artificial equilibrium on the background trend. This will particularly affect the deep ocean, which takes much longer to respond to changes in forcing than the upper ocean. This is consistent with the thermal expansion estimates presented in Table 3, where the full-depth thermal expansion in the observations is underestimated by the modeled estimates, in contrast to the 0–700-m thermal expansion. We therefore propose to use a nonequilibrium constant to account for a combined ongoing ice sheet/deep ocean contribution in the twentieth century (Fig. 6). A value of 0.13 ± 0.35 mm yr^{-1} was derived in Slangen et al. (2016) using CMIP5 thermal expansion (CMIP5 variable zostoga) compared to observed thermal expansion (the same estimates as used in this study) for the period 1970–2005 (see their supplementary Fig. S2 for the derivation).

d. Terrestrial water storage change

Water is continuously being transferred between the ocean and land as part of the natural hydrological cycle and partly due to human intervention. While natural terrestrial water exchange, such as snowfall or surface water storage, is assumed to be in equilibrium on longer (from decadal to century) time scales (Church et al. 2013a; Wada et al. 2017), processes such as groundwater extraction and reservoir building can have a long-lasting effect on GMSL. People extract groundwater from deep reservoirs, to use for instance as drinking water, for industries, and to irrigate the land, bringing additional water into the active hydrological cycle and into the ocean. On the other hand, dams and reservoirs are built in rivers, leading to additional storage of water on land and a reduction of water flowing into the ocean.

However, these processes are not included in the climate models. Therefore, we use observation-based estimates of the twentieth-century contributions to GMSL from groundwater extraction and reservoir

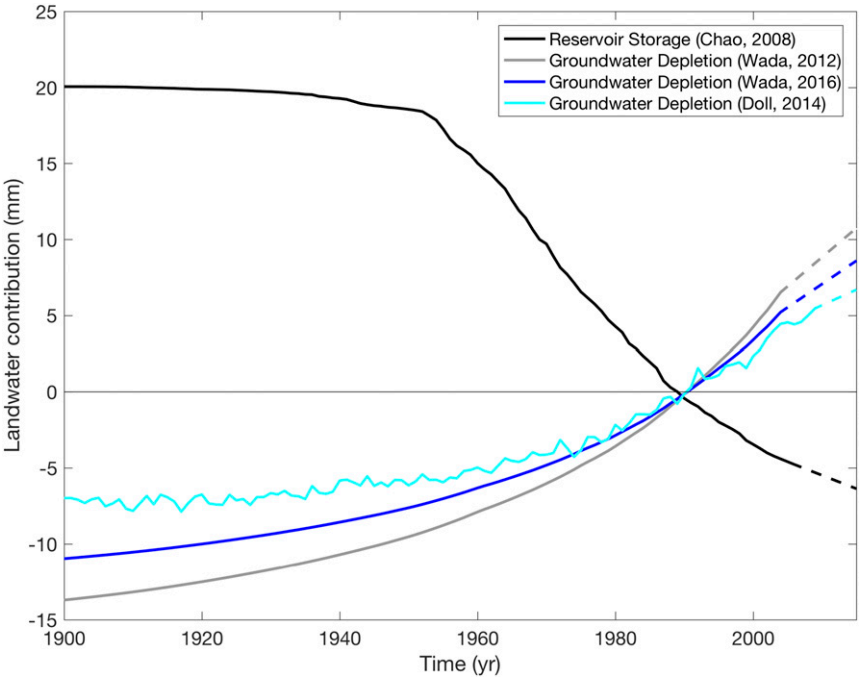

FIG. 7. Landwater storage change contributions to sea level change (1900–2015; mm), relative to a baseline period of 1980–2000. Dashed lines indicate extension of time series to 2015 using the average rate of the last 5 years of available data.

building. For water storage behind dams, we use the Chao et al. (2008) estimate (1900–2007), scaled by 0.85 of the nominal storage capacity as suggested in IPCC AR5 (Church et al. 2013b). We use two estimates for groundwater depletion. The first comes from Wada et al. (2012) for 1900–2005, corrected for recent findings in Wada et al. (2016), showing that only 80% of the depleted groundwater ends up in the ocean. This brings their estimate closer to earlier estimates that also reflected smaller contributions to GMSL from groundwater extraction (e.g., Konikow 2011). Wada et al. (2012, 2016) used a global hydrological model to compute groundwater depletion using country-specific groundwater abstraction data, but they did not model the reduction in base flow due to groundwater abstraction. The second estimate, from Döll et al. (2014), is available from 1902 to 2009 and presents a smaller contribution than that of Wada et al. (2012, 2016). They used a different hydrological model, which computes the change in groundwater storage from the difference between groundwater abstraction and recharge, including a decline in base flow as the storage decreases. Both groundwater depletion time series, as well as the reservoir storage time series, were extended to 2015 using the average rate in the last 5 years of available data.

The rates of change for reservoir storage and groundwater extraction are small before 1950 (Fig. 7). The reservoir storage then sharply increases, leading to sea level fall, and starts tapering off toward the end of the century because dam construction declined. Both groundwater estimates show a more gradual acceleration after 1950, with most of the increase toward the end of the period, contributing to sea level rise throughout the century. The reservoir storage (-25 mm from 1901–20 to 1996–2015) is larger than the groundwater contribution of 16 mm for the same period from Wada et al. (2012, 2016) and 11 mm for Döll et al. (2014). This study uses the average of the studies of Wada and Döll as the groundwater estimate, and the difference between the two groundwater studies (5 mm) is used as the 1σ uncertainty estimate for the landwater storage change component. Combined with the reservoir storage, this leads to an overall GMSL change of -11 ± 7 mm (1.65σ) from 1901–20 to 1996–2015.

4. Modeled sea level change compared to observations and reconstructions

a. The twentieth century to present day (1900–2015)

For the whole of the twentieth century, glacier mass loss and ocean thermal expansion are the largest contributors to GMSL (Fig. 8, Table 4). The proposed correction to the early-twentieth-century glacier contribution (section 3b) makes the glaciers the largest contributor in

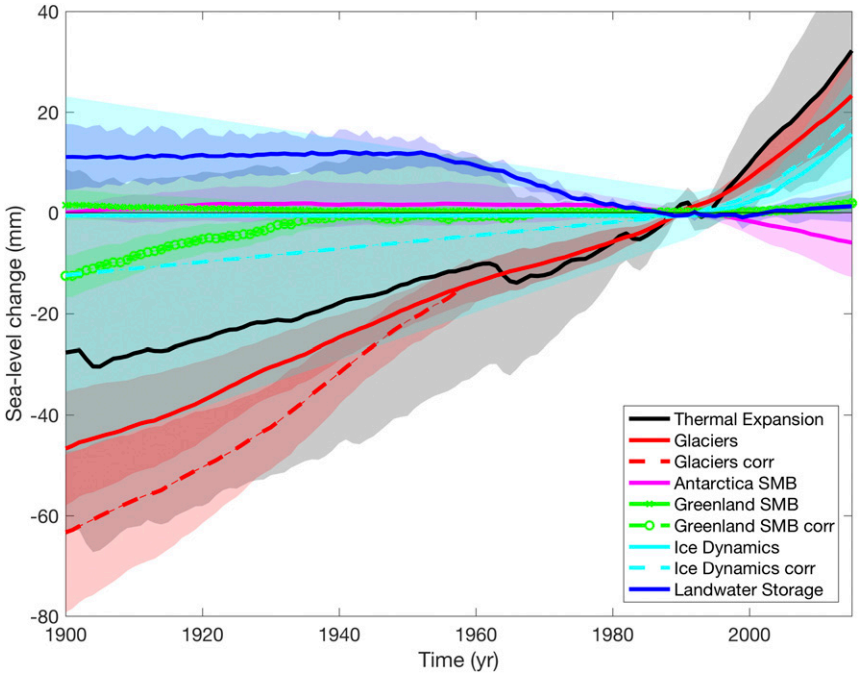

FIG. 8. Modeled sea level contributions (1900–2015; mm) ensemble mean $\pm 1.65\sigma$ for each contribution, relative to a baseline period of 1980–2000, excluding (solid) and including (dashed) proposed corrections.

the beginning of the century, whereas from the middle of the century onward the thermal expansion accelerates faster than the glaciers. Both contributions show a change in pace around the 1990s (Fig. 8). From 1900 to 1990 the thermal expansion contributes approximately 30 mm in 90 years, which is the same amount as in the 25 years after 1990. This agrees with observational estimates of the increase in ocean heat content in the twentieth century (Gleckler et al. 2016). The change in pace is a result of the recovery after the Pinatubo eruption, as well as increasing greenhouse gas concentrations in tandem with decreasing anthropogenic aerosol concentrations (Gleckler et al. 2006; Slangen et al. 2014b). The glaciers contributed 50 mm (65 mm including the proposed corrections) in the first 90 years and about 25 mm in the last 25 years, doubling their rate of change. The landwater contribution causes a sea level fall before the 1950s due to the increasing reservoir storage, while closer to the present day the groundwater extraction increases, leading to a small and increasing positive contribution to GMSL from landwater storage changes. The ice sheet SMB contributions are relatively small compared to all the other contributions, apart from the proposed bias correction to the Greenland SMB component, which is of similar magnitude (but opposite sign) as the landwater storage change. Finally, the ice sheet dynamical component is initially dominated by the proposed nonequilibrium term, but by the end of the century the ice sheets start to show an increasing contribution from ice sheet dynamical discharge.

When all the contributions are combined, the models add up to a GMSL change of 92 ± 47 mm for the period from 1901–20 to 1996–2015 (Table 4, Fig. 9a). Compared to the average of the four reconstructed global mean time series for the overlapping period from 1901–20 to 1988–2007 (Table 5, Fig. 9a, the model simulations clearly underestimate the observed GMSL and explain only 50% ± 30% of the observed change (using $\pm 1.65\sigma$ of the models to the mean of the observations). For the individual reconstructions, the explained percentages range from 43% (Jevrejeva et al. 2014) to 61% (Hay et al. 2015). These low percentages are mainly due to differences in the earlier part of the century, whereas the percentages significantly increase for later periods (see section 4b).

If the proposed corrections are added to the model simulations, the simulations explain a larger percentage of 75% ± 38% of the averaged reconstructed changes (Fig. 9b), with the lowest explained percentage being 65% (Jevrejeva et al. 2014) and the highest 92% (Hay et al. 2015). The increased percentages after adding the corrections indicate that the component biases (between models and observations of individual contributions) are

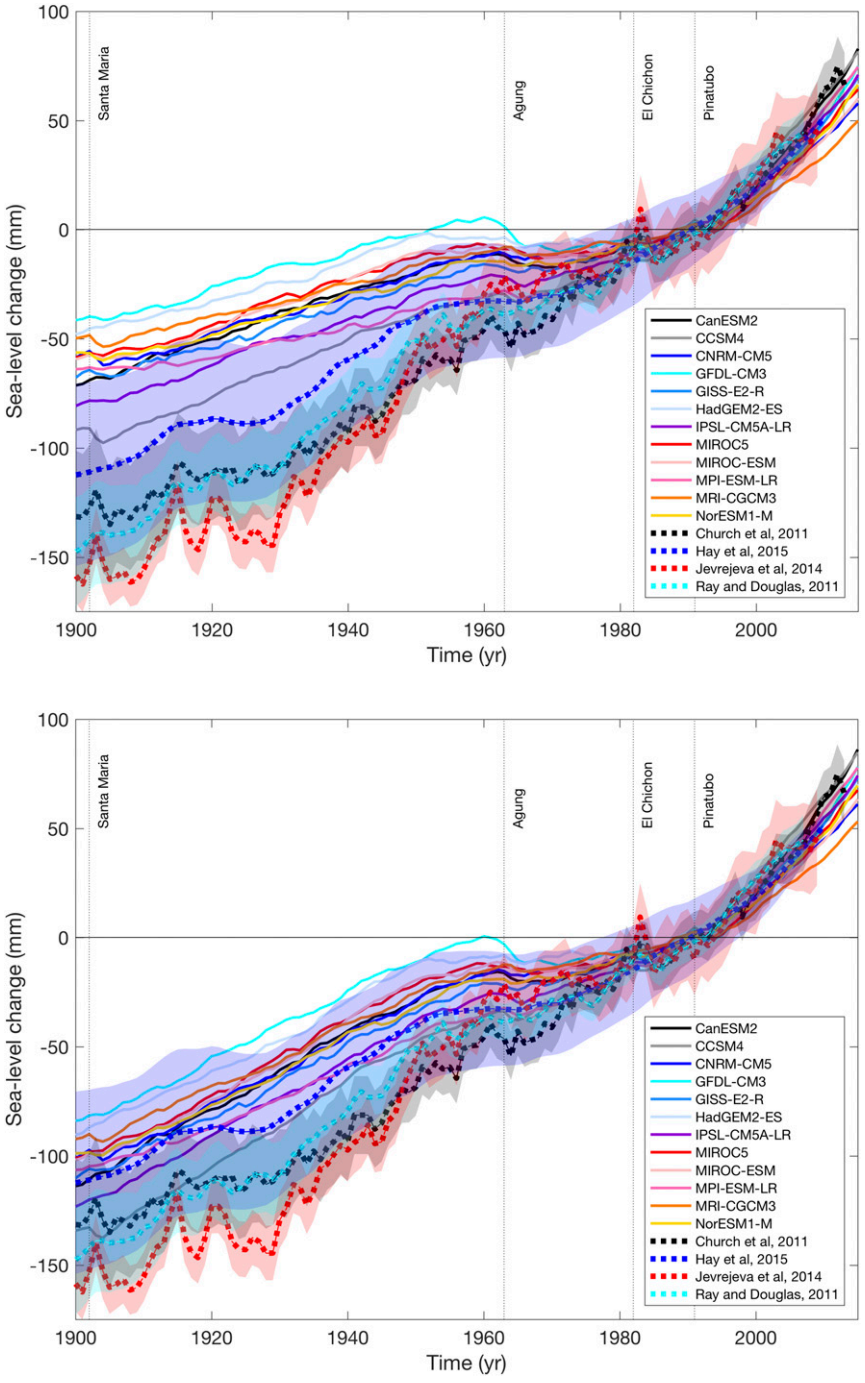

FIG. 9. Modeled total sea level change (1900–2015; mm) for 12 CMIP5 models compared to observational reconstructions, relative to a baseline period of 1980–2000, showing models (a) excluding and (b) including proposed corrections for glaciers and ice sheets. Observational reconstructions (dashed lines) are Church and White (2011) in gray, Hay et al. (2015) in blue, Jevrejeva et al. (2014) in red, Ray and Douglas (2011) in cyan; shading indicates 1.65σ. Major volcanic eruptions are indicated with dashed vertical lines.

TABLE 5. Comparing models and tide gauge reconstructions for the period from 1901–20 to 1988–2007 (mm ± 1.65σ).

	GMSL change (mm) from 1901–20 to 1988–2007
Obs (Church and White 2011)	138 ± 24
Obs (Hay et al. 2015)	115 ± 39
Obs (Jevrejeva et al. 2014)	163 ± 12
Obs (Ray and Douglas 2011)	148 ± 20
Mean obs	141 ± 51
Total models (excluding correction)	70 ± 42
Total models (including correction)	106 ± 53

consistent with the total sea level bias and that improvements are needed in the simulation of mass terms in the early twentieth century to be able to close the sea level budget. With the corrections, the twentieth-century simulated budget falls within 1.65σ uncertainty of the tide gauge observations (Table 5) and nearly closes the budget for the Hay et al. (2015) reconstruction.

Both the models and the observations show a more or less linear increase before 1950, followed by a short plateau, before starting to accelerate toward the present day (Fig. 9). However, the year-to-year variability in the observations is much larger than in the simulations, which show little variability apart from the response to volcanic eruptions. This may be explained by the fact that observations contain much more small-scale "noise." The relatively large variability in the sparsely distributed observations tends to lead to an overestimate of the interannual variability in the global mean, as shown by comparisons between tide gauge reconstructions and satellite altimetry (Church and White 2011; Meyssignac et al. 2012). On the other hand, the variability in the climate model global mean may be underestimated because of processes that are either underestimated or absent from the climate models. Reasons for this could be the relatively coarse (ocean and atmospheric) grids of the models (both in latitude/longitude and in depth), which require parameterizations of subgrid-scale processes, such as eddies (e.g., Hallberg 2013) or turbulence (e.g., Melet et al. 2016).

b. *The satellite era (1993–2015)*

In the satellite era (1993–2015) the thermal expansion is the largest contribution, followed by the glaciers and the ice dynamic contribution (Fig. 10).This is different compared to the whole of the century (Fig. 8), where the ice sheet dynamics without the nonequilibrium correction were small: this contribution only starts to contribute from the 1990s onward. The landwater contribution in the satellite era is small, as the reservoir storage and the groundwater extraction largely cancel each other out. The Antarctic SMB contribution on its own would cause a sea level fall due to the increased snowfall on the ice sheet as a result of warmer air temperatures. Most

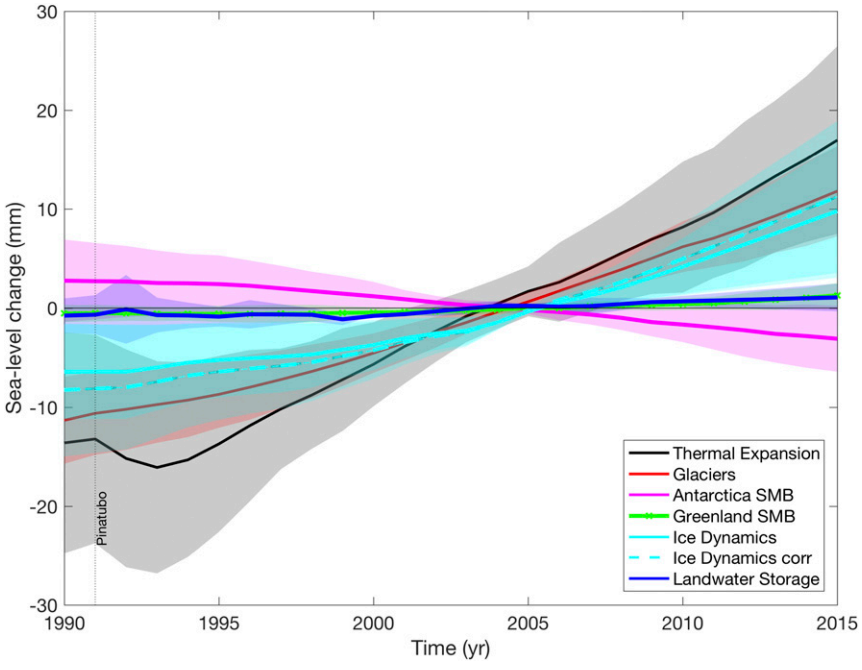

FIG. 10. Modeled sea level contributions (1990–2015; mm), ensemble mean ±1.65σ for each contribution, relative to a baseline period of 1993–2015 (the satellite era), excluding (solid) and including (dashed) the proposed nonequilibrium correction.

TABLE 6. Comparing models and satellite observations for the period from 1993–97 to 2011–15 (mm ± 1.65σ).

	GMSL change (mm) from 1993–97 to 2011–15
Obs (ESA-CCI)	59
Obs (CSIRO)	59
Obs (Watson et al. 2015)	47
Mean Obs	55
Total models (excluding correction)	56 ± 18
Total models (including correction)	58 ± 19

contributions, apart from the Antarctic SMB, show a more or less linear increase for 1993–2015. As we saw in the previous section, both the thermal expansion and glacier contributions have increased significantly in these last 25 years compared to earlier in the twentieth century, doubling to tripling the contributions in recent times. The thermal expansion contribution shows a temporary response to the 1991 Pinatubo eruption for the two consecutive years but resumes a linear increase from 1993 onward.

Combined, the simulated GMSL change from 1993–97 to 2011–15 is 56 ± 18 mm (Table 6). The observations (tide gauges and satellites) and model estimates are much closer to each other over this more recent period than they were for the full twentieth century (cf. Figs. 11 and 9), agreeing well with a recent review study on the sea level budget during the altimetry era by Chambers et al. (2017). Also, the proposed corrections have a much smaller influence for this period than over the twentieth century, as the corrections due to early-twentieth-century warming around Greenland have no impact after 1970, and only the nonequilibrium contribution is still included. This leads to a modeled change of 58 ± 19 mm over the altimetry period (from 1993–97 to 2011–15), which is only 2 mm larger than the uncorrected model estimate. Since this is a relatively short period, and the averages are only taken over 5 years, one should keep in mind that internal climate variability may influence these values. The two satellite altimetry time series from ESA-CCI and CSIRO find nearly the same change from 1993–97 to 2011–15 (Table 6).

We also compare the models to the recently published satellite time series of Watson et al. (2015), who proposed to calibrate the satellite record with GPS-corrected tide gauges in an attempt to remove a possible bias drift in the first part of the altimeter record. This is in contrast to the treatment of the other two satellite time series above, which are completely independent from tide gauge estimates. The Watson et al. (2015) satellite time series has a smaller GMSL change than the other two estimates and

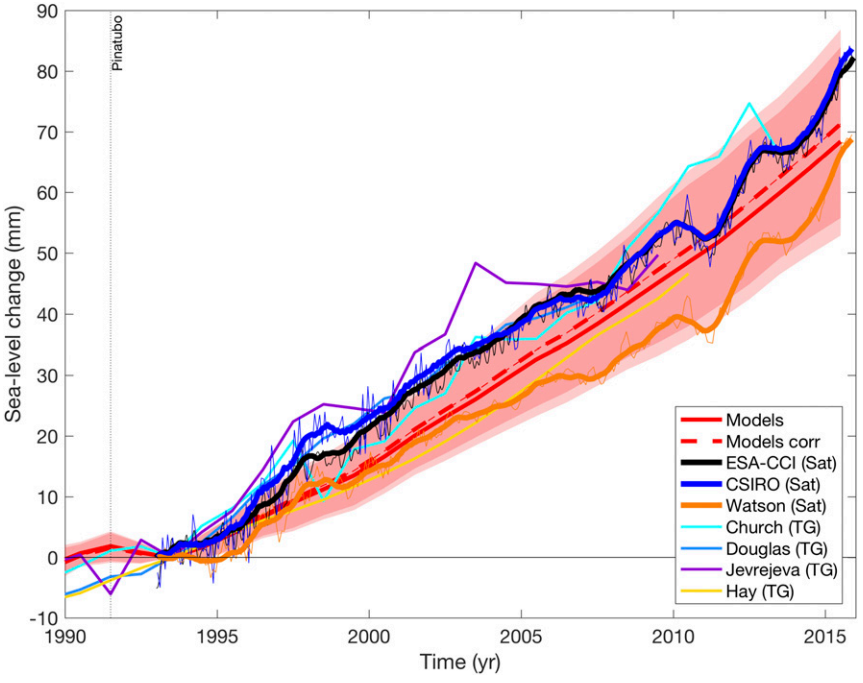

FIG. 11. Modeled total sea level change (1990–2015; mm; ±1.65σ) for the ensemble of 12 CMIP5 models (red solid line excluding and red dashed line including proposed nonequilibrium correction; annual values placed on center of year) compared to satellite altimetry [ESA-CCI, CSIRO, and Watson et al. (2015); annual running mean in thick, monthly data in thin lines] and tide gauge reconstructions (annual values), all time series plotted relative to the year 1993.

less than the model ensemble means (Table 6) but is still within the model uncertainty range.

Over the satellite period, the model simulations explain 102% ± 33% of the satellite observations [Table 6; mean of the three satellite estimates, 95% for CSIRO, 95% for ESA-CCI, and 119% for Watson et al. (2015)]. When proposed corrections are included the percentages increase to 105% ± 35% [98% for CSIRO, 98% for ESA-CCI, and 123% for Watson et al. (2015)]. The percentages for both the uncorrected and the corrected simulations of the satellite period show a significant improvement compared to the whole of the twentieth century. Although there is a much smaller impact of the proposed corrections for this more recent period, they still improve the budget closure.

c. *Increases in trends and changes in relative contributions to twentieth-century sea level rise*

The yearly trends, averaged over 10 years (Fig. 12a), in simulated GMSL over the twentieth century are increasing from 0.7 mm yr^{-1} for 10 decades centered on 1904–13 to 3.2 mm yr^{-1} for 10 decades centered on 2001–10, and increase from 1.4 to 3.4 mm yr^{-1} for the corrected simulations. This is due to increasing trends in both the thermal expansion (from 0.2 to 1.4 mm yr^{-1}) and the combined mass component of glaciers, ice sheets, and landwater (from 0.5 to 1.8 mm yr^{-1} for uncorrected and from 1.2 to 2.0 mm yr^{-1} corrected simulations). The increase in thermal expansion is consistent with Earth's energy imbalance of the last decades, as a result of the long-term increase in radiative forcing associated with increased greenhouse gas emissions (Smith et al. 2015; von Schuckmann et al. 2016).

The 10-yr averaged trends in the observations also increase in the twentieth century, from 1.7 mm yr^{-1} (tide gauge trends 10-yr running means centered on 1904–13) to 2.9 mm yr^{-1} (satellite 10-yr running mean trends centered on 2001–10). The observations show 1 than the simulations (Fig. 12), but they fall within 1.65 standard deviations (1.65σ) of the model spread for most decades. The period of 1930–50 shows similar observed trends to the period 1990–2010, with the difference that in the more recent period the trends continue to increase rather than decrease as they did in 1950–60 (Fig. 12a). The difference is probably that in the beginning of the century the trends are driven by internal variability, whereas later in the century they are driven by external forcing (Slangen et al. 2016). However, part of the explanation could also be in the observations, which may have too much variability in the observations due to sparse spatial sampling (Church and White 2011; Meyssignac et al. 2012).

In the beginning of the twentieth century, the majority of the (simulated) GMSL comes from mass-driven contributions (i.e., glaciers, ice sheets, and landwater) rather than thermal expansion. This is enhanced when the mass bias corrections are included (Figs. 12b,c). These early-twentieth-century changes have been attributed to natural forcing and internal climate variability (e.g., the glaciers' response to the end of the Little Ice Age and early-twentieth-century warming around Greenland) rather than anthropogenic forcing (Marzeion et al. 2014; Slangen et al. 2016). In contrast, for the late twentieth century (1991–2010), 69% ± 40% (±1.65σ) of the glacier contribution has been attributed to anthropogenic change (Marzeion et al. 2014), which clearly shows a shift from natural to anthropogenic forcing over the course of the twentieth century. Thermal expansion responds differently to external forcing: it starts to contribute positively to GMSL from 1910 onward and by 2015 is responsible for 46% of the cumulative simulated GMSL change since 1900 (34% of the corrected simulations). This contribution is mainly attributable to anthropogenic forcing (>80% since 1970; Marcos and Amores 2014; Slangen et al. 2014a). When the thermal expansion and mass contributions are combined, the majority of GMSL change since 1970 (69% ± 26%; ±1.65σ) is attributable to anthropogenic forcing (Slangen et al. 2016).

The mass term contributes positively to GMSL throughout the twentieth century (even though some individual mass contributions such as landwater storage can be negative contributors), but its *relative* contribution decreases as thermal expansion increases (Fig. 12c). Initially, the mass contribution almost entirely consists of the glacier contribution (and Greenland SMB when the bias corrections are included), but the *relative* contribution from glaciers decreases from 1993 onward. The relative ice dynamical contribution (included in the mass contribution) starts from 1993, accounts for 12% of the cumulative change by 2015 (18% when corrections are included), and is rapidly increasing over the period 1993–2015. Although both the mass terms and the thermal expansion are increasingly contributing to GMSL in an absolute sense (Figs. 12a,b), their relative contributions have stabilized from 2000 onward (Fig. 12c), indicating that the increase in the thermal expansion and the increase in the mass contributions are following the same pace for now. As the future changes in the ice sheets are still quite uncertain, in particularly the contribution of the Antarctic ice sheet (Church et al. 2013a; Slangen et al. 2014a; Kopp et al. 2014; Ritz et al. 2015; DeConto and Pollard 2016), the relative contributions may change if the mass contribution overtakes the thermal expansion contribution.

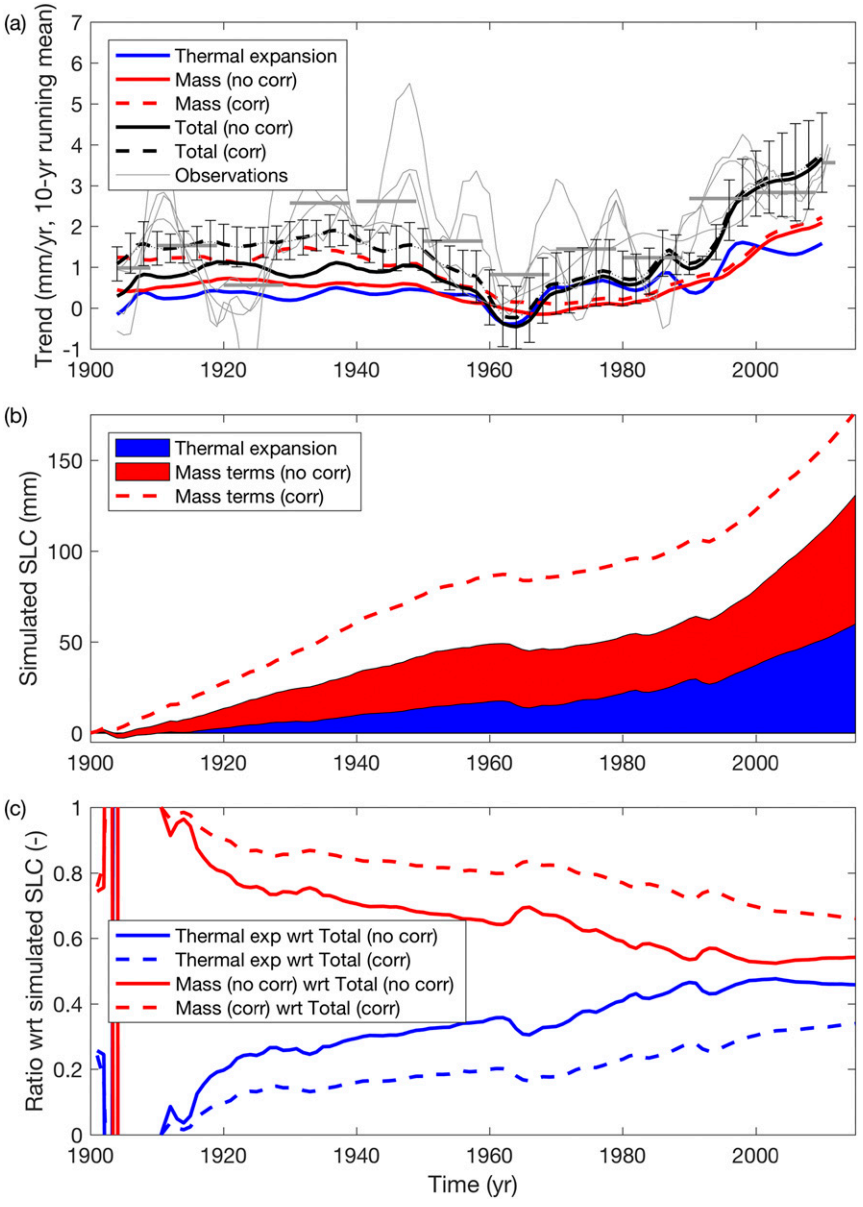

FIG. 12. Twentieth-century sea level change, comparing thermal expansion to the summed mass contributions (glaciers, ice sheets, and landwater), to the total simulated contributions (a) trends in observations (10-yr running mean of yearly trends in all tide gauge reconstructions and satellite time series, and bars indicating the decadal mean of all observations) and model simulations (10-yr running mean of yearly trends; error bars indicate 1.65σ uncertainties for total-corrected simulations) (mm yr^{-1}); (b) stacked cumulative contributions of thermal expansion and mass terms to total simulated sea level rise since 1900 (mm); and (c) relative contributions of thermal expansion and mass terms to total simulated sea level rise since 1900. Spikes in first decade are a result of taking ratios of very small values and switching between positive and negative after the 1903 Santa María eruption.

5. Discussion and conclusions

In this paper, we focused on evaluating twentieth-century observed GMSL change using model estimates. To get a consistent dataset, we have used the same 12 climate models' data output to estimate the contributions of thermal expansion (assuming salinity change is negligible in the global mean), glaciers and ice sheet SMB, to GMSL. The simulated GMSL is completed by adding observation-based estimates of ice sheet

dynamical processes and landwater storage changes. We use four sets of tide gauge reconstructions and three satellite altimetry time series to compare our model estimates to. With respect to previous comparisons (Church et al. 2013b; Slangen et al. 2016), we have extended the evaluation period up to 2015 using the RCP8.5 climate model scenario, and we use a consistent climate model ensemble, which allows us to evaluate individual climate model results.

Other differences with respect to IPCC AR5 and previous model–observation comparisons (Church et al. 2013a,b; Slangen et al. 2016) are in the individual contributions, where recent findings and model updates change some of the estimates, and different approaches were used to compute the ice sheet contributions. This leads to more consistent and robust estimates of the contributions to GMSL. The glacier contribution, for instance, contains an updated glacier inventory and improvements to the digital elevation model, which have caused a decrease in the CMIP5 estimated twentieth-century glacier contribution compared to the IPCC AR5 results (Marzeion et al. 2015).

The contributions of the Greenland and Antarctic ice sheets are a combination of increases in the runoff of surface meltwater, enhanced calving of solid ice, and melting of ice that is in contact with the ocean, with the former process dominating in Greenland and the latter two in Antarctica. Here, we use different methods to estimate these contributions, using CMIP5 data where possible to obtain a consistent dataset, an improvement with respect to previous work. At present, there are no models that we are aware of that simulate a robust and complete ice sheet in response to twentieth-century climate, but this is expected to change with the forthcoming CMIP6-endorsed Ice Sheet Model Intercomparison (ISMIP; Nowicki et al. 2016). As the future contribution of these ice sheets is expected to increase in a warming climate, such comprehensive simulations of the ice sheet contribution will be a significant contribution to the understanding of historical GMSL and evaluating our current understanding of GMSL and ice sheet models. Progress in these areas will lead to more robust projections of sea level change.

In addition, recent groundwater extraction estimates were used (e.g., Döll et al. 2014), which tend to be lower than the values included in IPCC AR5. This is in agreement with another recent publication, showing that only 80% of the extracted groundwater of Wada et al. (2012) ultimately reaches the ocean (Wada et al. 2016).

We furthermore suggest bias corrections for some of the GMSL contributions, based on differences between models and observations. For instance, observational evidence points to a much larger (SMB + ice dynamical) contribution from the Greenland ice sheet than previously thought (Kjeldsen et al. 2015). This is in line with the finding that the glacier contribution and the Greenland SMB contribution are much larger in the early twentieth century when they are computed using temperature reanalyses rather than CMIP5 model estimates (Slangen et al. 2016). In this study, we include a correction for the Greenland SMB contribution based on the differences between the CMIP5-driven results and the reanalysis driven results.

Following Slangen et al. (2016), we also explored the possibility that ice sheets and the deep ocean are not in equilibrium with twentieth-century climate by introducing a nonequilibrium constant, as their response time is likely to be on a century to millennia time scale. We use a constant of $0.13 \pm 0.35\,\mathrm{mm\,yr^{-1}}$ as derived in Slangen et al. (2016).

Throughout this study, all the modeled and observational glacier estimates discussed have excluded the contribution from the Antarctic peripheral glaciers (PGs), following the approach taken in IPCC AR5, as this is an extremely uncertain contribution. Observations of these glaciers are sparse and the mechanics are poorly understood: it is unclear whether they should be included in the glacier estimate or the Antarctic SMB estimate. For a rough estimate of the PG contribution, Marzeion et al. (2012) suggested to scale the total area of the PGs to the total global glacier area (minus PGs) to derive a scaling factor that can be used to scale the global glacier contribution with. This scaling factor of 0.22 ($132\,867/593\,925\,\mathrm{m^2}$) would result in an additional sea level contribution from the PGs of 12 mm from 1901–20 to 1996–2015, which would reduce the twentieth-century difference between observations and simulations. If the PG were assumed to follow the Antarctic SMB evolution the contribution would be much smaller, as the Antarctic contribution is small throughout the twentieth century. However, as the contribution is so poorly constrained, we have decided not to include this contribution in our simulated GMSL estimates.

When all the contributions are combined, there is still a large gap between the observations and the models, and only 50% ± 30% of the observations (mean of four tide gauge reconstructions) can be explained by the models for the period from 1901–20 to 1988–2007. The suggested bias corrections for Greenland SMB, glaciers, and deep ocean/ice sheet reduce the model–observation gap by construction, as they are based on model–observation differences, bringing the explained percentage to 75% ± 38% for the mean of the four reconstructions. Compared to the individual reconstructions, the bias-corrected simulations agree best with the Hay et al. (2015) reconstruction, explaining 92% of the observed change (Table 5).

For the more recent satellite period (from 1993 to 2015), the explained percentage (i.e., explained by the simulations) is 102% ± 33% (105% ± 35% when bias corrections are included), effectively closing the sea level budget for this period. In this later period, the uncertainties in the observations are smaller as the data resolution is higher, both spatially and temporally. The model uncertainties, mainly based on the spread between the different CMIP5 models (Table 4), are smaller in absolute sense for the later period, but the percentage remains the same, showing that the uncertainties in the models are relatively constant for the different periods.

The simulated GMSL time series shows increasing trends over the twentieth century due to increasing contributions from both thermal expansion and the mass components. Thermal expansion starts to contribute to GMSL from 1910 onward, and by 2015 accounts for 46% of the total simulated sea level rise. The mass contribution, which accounts for the remaining 54% in 2015, is dominated by the glacier contribution until the ice sheet dynamics start to play a role at the end of the twentieth century, accounting for 12% of total simulated GMSL in 2015.

In a warming climate, all of the contributions are expected to continue to increase in the coming century, with potentially the largest increase in the contributions from the ice sheets (Church et al. 2013a). Because of the delayed response in the deep ocean and ice sheets, sea level will continue to rise even if the emission of greenhouse gases were reduced today. It is therefore important to understand the response times and the magnitude of the different processes to better estimate future changes in sea level. This paper, presenting the GMSL budget, is a step forward in this process. The next step is to evaluate and understand regional patterns in sea level change as a result of these processes, which is done in the companion paper (M17).

Acknowledgments. This paper is an outcome of work with the ISSI international team on "Contemporary regional and global sea-level rise: assessment of satellite and in-situ observations and climate models." We thank ISSI (www.issibern.ch) for facilitating the team meetings. We acknowledge the World Climate Research Programme's Working Group on Coupled Modelling, which is responsible for CMIP, and we thank the climate modeling groups (listed in Table 1 of this paper) for producing and making available their model output. For CMIP, the U.S. Department of Energy's Program for Climate Model Diagnosis and Intercomparison provides coordinating support and leads development of software infrastructure in partnership with the Global Organization for Earth System Science Portal. We thank P. Leclercq (U. Oslo) for providing the updated glacier contribution based on glacier length records. A.S. received funding from a CSIRO Office of the Chief Executive postdoctoral fellowship and the NWO-Netherlands Polar Programme. M.P. and C.R. were supported by the Joint UK BEIS/Defra Met Office Hadley Centre Climate Programme (GA01101). In the early part of this study, J.C. was funded by CSIRO, the Australian Climate Change Science Program, and the University of New South Wales. S.L. was supported by an NWO ALW Veni Grant (865.15.023). K.R. was supported by the Austrian Science Fund (FP253620).

REFERENCES

Ablain, M., and Coauthors, 2015: Improved sea level record over the satellite altimetry era (1993–2010) from the Climate Change Initiative project. *Ocean Sci.*, **11**, 67–82, doi:10.5194/os-11-67-2015.

Abraham, J. P., and Coauthors, 2013: A review of global ocean temperature observations: Implications for ocean heat content estimates and climate change. *Rev. Geophys.*, **51**, 450–483, doi:10.1002/rog.20022.

Arendt, A. A., A. Bliss, T. Bolch, and J. G. Cogley, 2014: Randolph glacier inventory—A dataset of global glacier outlines. Version 4.0. Global Land Ice Measurements from Space (GLIMS) Tech. Rep., 56 pp. [Available online at www.glims.org/RGI/00_rgi40_TechnicalNote.pdf.]

Bentsen, M., and Coauthors, 2013: The Norwegian Earth System Model, NorESM1-M—Part 1: Description and basic evaluation of the physical climate. *Geosci. Model Dev.*, **6**, 687–720, doi:10.5194/gmd-6-687-2013.

Bjørk, A. A., and Coauthors, 2012: An aerial view of 80 years of climate-related glacier fluctuations in southeast Greenland. *Nat. Geosci.*, **5**, 427–432, doi:10.1038/ngeo1481.

Box, J. E., L. Yang, D. H. Bromwich, and L.-S. Bai, 2009: Greenland Ice Sheet surface air temperature variability: 1840–2007. *J. Climate*, **22**, 4029–4049, doi:10.1175/2009JCLI2816.1.

Boyer, T., and Coauthors, 2016: Sensitivity of global upper-ocean heat content estimates to mapping methods, XBT bias corrections, and baseline climatologies. *J. Climate*, **29**, 4817–4842, doi:10.1175/JCLI-D-15-0801.1.

Cannaby, H., and Coauthors, 2016: Projected sea level rise and changes in extreme storm surge and wave events during the 21st century in the region of Singapore. *Ocean Sci.*, **12**, 613–632, doi:10.5194/os-12-613-2016.

Cazenave, A., N. Champollion, F. Paul, and J. Benveniste, Eds., 2017: *Integrative Study of the Mean Sea Level and Its Components*. Springer, 416 pp.

Chambers, D. P., A. Cazenave, N. Champollion, H. Dieng, W. Llovel, R. Forsberg, K. von Schuckmann, and Y. Wada, 2017: Evaluation of the global mean sea level budget between 1993 and 2014. *Surv. Geophys.*, **38**, 309–327, doi:10.1007/s10712-016-9381-3.

Chao, B. F., Y. H. Wu, and Y. S. Li, 2008: Impact of artificial reservoir water impoundment on global sea level. *Science*, **320**, 212–214, doi:10.1126/science.1154580.

Cheng, L., K. E. Trenberth, M. D. Palmer, J. Zhu, and J. P. Abraham, 2016: Observed and simulated full-depth ocean heat-content changes for 1970–2005. *Ocean Sci.*, **12**, 925–935, doi:10.5194/os-12-925-2016.

——, ——, J. Fasullo, T. Boyer, J. Abraham, and J. Zhu, 2017: Improved estimates of ocean heat content from 1960 to 2015. *Sci. Adv.*, **3**, e1601545, doi:10.1126/sciadv.1601545.

Church, J. A., and N. J. White, 2006: A 20th century acceleration in global sea-level rise. *Geophys. Res. Lett.*, **33**, L01602, doi:10.1029/2005GL024826.

——, and ——, 2011: Sea-level rise from the late 19th to the early 21st century. *Surv. Geophys.*, **32**, 585–602, doi:10.1007/s10712-011-9119-1.

——, and Coauthors, 2011: Revisiting the Earth's sea-level and energy budgets from 1961 to 2008. *Geophys. Res. Lett.*, **38**, L18601, doi:10.1029/2011GL048794.

——, and Coauthors, 2013a: Sea level change. *Climate Change 2013: The Physical Science Basis*, T. F. Stocker et al., Eds., Cambridge University Press, 1137–1216.

——, D. Monselesan, J. M. Gregory, and B. Marzeion, 2013b: Evaluating the ability of process based models to project sea-level change. *Environ. Res. Lett.*, **8**, 014051, doi:10.1088/1748-9326/8/1/014051.

Cogley, J. G., 2009: Geodetic and direct mass-balance measurements: Comparison and joint analysis. *Ann. Glaciol.*, **50**, 96–100.

Compo, G. P., and Coauthors, 2011: The Twentieth Century Reanalysis Project. *Quart. J. Roy. Meteor. Soc.*, **137**, 1–28, doi:10.1002/qj.776.

DeConto, R. M., and D. Pollard, 2016: Contribution of Antarctica to past and future sea-level rise. *Nature*, **531**, 591–597, doi:10.1038/nature17145.

Döll, P., H. Müller Schmied, C. Schuh, F. T. Portmann, and A. Eicker, 2014: Global-scale assessment of groundwater depletion and related groundwater abstractions: Combining hydrological modeling with information from well observations and GRACE satellites. *Water Resour. Res.*, **50**, 5698–5720, doi:10.1002/2014WR015595.

Domingues, C. M., J. A. Church, N. J. White, P. J. Gleckler, S. E. Wijffels, P. M. Barker, and J. R. Dunn, 2008: Improved estimates of upper-ocean warming and multi-decadal sea-level rise. *Nature*, **453**, 1090–1094, doi:10.1038/nature07080.

Dufresne, J. L., and Coauthors, 2013: Climate change projections using the IPSL-CM5 Earth System Model: From CMIP3 to CMIP5. *Climate Dyn.*, **40**, 2123–2165, doi:10.1007/s00382-012-1636-1.

Enderlin, E. M., I. M. Howat, S. Jeong, M.-J. Noh, J. H. van Angelen, and M. R. van den Broeke, 2014: An improved mass budget for the Greenland ice sheet. *Geophys. Res. Lett.*, **41**, 866–872, doi:10.1002/2013GL059010.

Fettweis, X., B. Franco, M. Tedesco, J. H. van Angelen, J. T. M. Lenaerts, M. R. van den Broeke, and H. Gallee, 2013: Estimating the Greenland ice sheet surface mass balance contribution to future sea level rise using the regional atmospheric climate model MAR. *Cryosphere*, **7**, 469–489, doi:10.5194/tc-7-469-2013.

——, and Coauthors, 2017: Reconstructions of the 1900–2015 Greenland ice sheet surface mass balance using the regional climate MAR model. *Cryosphere*, **11**, 1015–1033, doi:10.5194/tc-11-1015-2017.

Frieler, K., and Coauthors, 2015: Consistent evidence of increasing Antarctic accumulation with warming. *Nat. Climate Change*, **5**, 348–352, doi:10.1038/nclimate2574.

Gent, P. R., and Coauthors, 2011: The Community Climate System Model version 4. *J. Climate*, **24**, 4973–4991, doi:10.1175/2011JCLI4083.1.

Giorgetta, M. A., and Coauthors, 2013: Climate and carbon cycle changes from 1850 to 2100 in MPI-ESM simulations for the Coupled Model Intercomparison Project phase 5. *J. Adv. Model. Earth Syst.*, **5**, 572–597, doi:10.1002/jame.20038.

Gleckler, P. J., K. AchutaRao, J. M. Gregory, B. D. Santer, K. E. Taylor, and T. M. L. Wigley, 2006: Krakatoa lives: The effect of volcanic eruptions on ocean heat content and thermal expansion. *Geophys. Res. Lett.*, **33**, L17702, doi:10.1029/2006GL026771.

——, P. J. Durack, R. J. Stouffer, G. C. Johnson, and C. E. Forest, 2016: Industrial-era global ocean heat uptake doubles in recent decades. *Nat. Climate Change*, **6**, 394–398, doi:10.1038/nclimate2915.

Gregory, J. M., 2010: Long-term effect of volcanic forcing on ocean heat content. *Geophys. Res. Lett.*, **37**, L22701, doi:10.1029/2010GL045507.

——, and Coauthors, 2013a: Twentieth-century global-mean sea level rise: Is the whole greater than the sum of the parts? *J. Climate*, **26**, 4476–4499, doi:10.1175/JCLI-D-12-00319.1.

——, and Coauthors, 2013b: Climate models without preindustrial volcanic forcing underestimate historical ocean thermal expansion. *Geophys. Res. Lett.*, **40**, 1600–1604, doi:10.1002/grl.50339.

Griffies, S. M., and Coauthors, 2011: The GFDL CM3 coupled climate model: Characteristics of the ocean and sea ice simulations. *J. Climate*, **24**, 3520–3544, doi:10.1175/2011JCLI3964.1.

Hallberg, R., 2013: Using a resolution function to regulate parameterizations of oceanic mesoscale eddy effects. *Ocean Modell.*, **72**, 92–103, doi:10.1016/j.ocemod.2013.08.007.

Harig, C., and F. J. Simons, 2015: Accelerated West Antarctic ice mass loss continues to outpace East Antarctic gains. *Earth Planet. Sci. Lett.*, **415**, 134–141, doi:10.1016/j.epsl.2015.01.029.

Harris, I., P. D. Jones, T. J. Osborn, and D. H. Lister, 2014: Updated high-resolution grids of monthly climatic observations—The CRU TS3.10 dataset. *Int. J. Climatol.*, **34**, 623–642, doi:10.1002/joc.3711.

Hay, C. C., E. Morrow, R. E. Kopp, and J. X. Mitrovica, 2015: Probabilistic reanalysis of twentieth-century sea-level rise. *Nature*, **517**, 481–484, doi:10.1038/nature14093.

Henry, O., M. Ablain, B. Meyssignac, A. Cazenave, D. Masters, S. Nerem, and G. Garric, 2014: Effect of the processing methodology on satellite altimetry-based global mean sea level rise over the Jason-1 operating period. *J. Geod.*, **88**, 351–361, doi:10.1007/s00190-013-0687-3.

Hobbs, W., M. Palmer, and D. Monselesan, 2016: An energy conservation analysis of ocean drift in the CMIP5 global coupled models. *J. Climate*, **29**, 1639–1653, doi:10.1175/JCLI-D-15-0477.1.

Ishii, M., and M. Kimoto, 2009: Reevaluation of historical ocean heat content variations with time-varying XBT and MBT depth bias corrections. *J. Oceanogr.*, **65**, 287–299, doi:10.1007/s10872-009-0027-7.

Jevrejeva, S., J. C. Moore, A. Grinsted, A. P. Matthews, and G. Spada, 2014: Trends and acceleration in global and regional sea levels since 1807. *Global Planet. Change*, **113**, 11–22, doi:10.1016/j.gloplacha.2013.12.004.

——, A. Matthews, and A. Slangen, 2017: The twentieth-century sea level budget: Recent progress and challenges. *Surv. Geophys.*, **38**, 295–307, doi:10.1007/s10712-016-9405-z.

Kjeldsen, K. K., and Coauthors, 2015: Spatial and temporal distribution of mass loss from the Greenland Ice Sheet since AD 1900. *Nature*, **528**, 396–400, doi:10.1038/nature16183.

Konikow, L. F., 2011: Contribution of global groundwater depletion since 1900 to sea-level rise. *Geophys. Res. Lett.*, **38**, L17401, doi:10.1029/2011GL048604.

Kopp, R. E., R. M. Horton, C. M. Little, X. Jerry, M. Oppenheimer, D. J. Rasmussen, B. H. Strauss, and C. Tebaldi, 2014: Probabilistic 21st and 22nd century sea-level projections at a global network of tide gauge sites. *Earth's Future*, **2**, 383–407, doi:10.1002/2014EF000239.

Leclercq, P. W., J. Oerlemans, and J. G. Cogley, 2011: Estimating the glacier contribution to sea-level rise for the period 1800–2005. *Surv. Geophys.*, **32**, 519–535, doi:10.1007/s10712-011-9121-7.

Lenaerts, J. T. M., M. R. van den Broeke, W. J. van de Berg, E. van Meijgaard, and P. K. K. Munneke, 2012: A new, high-resolution surface mass balance map of Antarctica (1979–2010) based on regional atmospheric climate modeling. *Geophys. Res. Lett.*, **39**, L04501, doi:10.1029/2011GL050713.

Levitus, S., and Coauthors, 2012: World ocean heat content and thermosteric sea level change (0–2000 m), 1955–2010. *Geophys. Res. Lett.*, **39**, L10603, doi:10.1029/2012GL051106.

Ligtenberg, S. R. M., W. J. van de Berg, M. R. van den Broeke, J. G. L. Rae, and E. van Meijgaard, 2013: Future surface mass balance of the Antarctic ice sheet and its influence on sea level change, simulated by a regional atmospheric climate model. *Climate Dyn.*, **41**, 867–884, doi:10.1007/s00382-013-1749-1.

Lowe, J. A., and J. M. Gregory, 2006: Understanding projections of sea level rise in a Hadley Centre coupled climate model. *J. Geophys. Res.*, **111**, C11014, doi:10.1029/2005JC003421.

Marcos, M., and A. Amores, 2014: Quantifying anthropogenic and natural contributions to thermosteric sea level rise. *Geophys. Res. Lett.*, **41**, 2502–2507, doi:10.1002/2014GL059766.

Martin, G. M., and Coauthors, 2011: The HadGEM2 family of Met Office Unified Model climate configurations. *Geosci. Model Dev.*, **4**, 723–757, doi:10.5194/gmd-4-723-2011.

Marzeion, B., A. H. Jarosch, and M. Hofer, 2012: Past and future sea-level change from the surface mass balance of glaciers. *Cryosphere*, **6**, 1295–1322, doi:10.5194/tc-6-1295-2012.

——, J. G. Cogley, K. Richter, and D. Parkes, 2014: Attribution of global glacier mass loss to anthropogenic and natural causes. *Science*, **345**, 919–921, doi:10.1126/science.1254702.

——, P. W. Leclercq, J. G. Cogley, and A. H. Jarosch, 2015: Brief communication: Global reconstructions of glacier mass change during the 20th century are consistent. *Cryosphere*, **9**, 2399–2404, doi:10.5194/tc-9-2399-2015.

——, N. Champollion, W. Haeberli, K. Langley, P. Leclercq, and F. Paul, 2017: Observation-based estimates of global glacier mass change and its contribution to sea-level change. *Surv. Geophys.*, **38**, 105–130, https://doi.org/10.1007/s10712-016-9394-y.

Masson-Delmotte, V. M., and Coauthors, 2013: Information from paleoclimate archives. *Climate Change 2013: The Physical Science Basis*, T. F. Stocker et al., Eds., Cambridge University Press, 383–464, doi:10.1017/CBO9781107415324.013.

Masters, D., R. S. Nerem, C. Choe, E. Leuliette, B. Beckley, N. White, and M. Ablain, 2012: Comparison of global mean sea level time series from TOPEX/Poseidon, Jason-1, and Jason-2. *Mar. Geod.*, **35**, 20–41, doi:10.1080/01490419.2012.717862.

McMillan, M., and Coauthors, 2016: A high-resolution record of Greenland mass balance. *Geophys. Res. Lett.*, **43**, 7002–7010, doi:10.1002/2016GL069666.

Melet, A., and B. Meyssignac, 2015: Explaining the spread in global mean thermosteric sea level rise in CMIP5 climate models. *J. Climate*, **28**, 9918–9940, doi:10.1175/JCLI-D-15-0200.1.

——, S. Legg, and R. Hallberg, 2016: Climatic impacts of parameterized local and remote tidal mixing. *J. Climate*, **29**, 3473–3500, doi:10.1175/JCLI-D-15-0153.1.

Meyssignac, B., M. Becker, W. Llovel, and A. Cazenave, 2012: An assessment of two-dimensional past sea level reconstructions over 1950–2009 based on tide-gauge data and different input sea level grids. *Surv. Geophys.*, **33**, 945–972, doi:10.1007/s10712-011-9171-x.

——, and Coauthors, 2017: Evaluating model simulations of twentieth-century sea level rise. Part II: Regional sea level change. *J. Climate*, **30**, 8565–8593, doi:10.1175/JCLI-D-17-0112.1.

Moss, R. H., and Coauthors, 2010: The next generation of scenarios for climate change research and assessment. *Nature*, **463**, 747–756, doi:10.1038/nature08823.

Munk, W., 2002: Twentieth century sea level: An enigma. *Proc. Natl. Acad. Sci. USA*, **99**, 6550–6555, doi:10.1073/pnas.092704599.

Nowicki, S. M. J., and Coauthors, 2016: Ice Sheet Model Intercomparison Project (ISMIP6) contribution to CMIP6. *Geosci. Model Dev.*, **9**, 4521–4545, doi:10.5194/gmd-2016-105.

Palmer, M. D., and Coauthors, 2010: Future observations for monitoring global ocean heat content. *Proc. OceanObs'09: Sustained Ocean Observations and Information for Society*, Vol. 2, Venice, Italy, European Space Agency, 740–751.

Poli, P., and Coauthors, 2016: ERA-20C: An atmospheric reanalysis of the twentieth century. *J. Climate*, **29**, 4083–4097, doi:10.1175/JCLI-D-15-0556.1.

Previdi, M., and Coauthors, 2016: Anthropogenic impact on Antarctic surface mass balance, currently masked by natural variability, to emerge by mid-century. *Environ. Res. Lett.*, **11**, 094001, doi:10.1088/1748-9326/11/9/094001.

Purkey, S. G., G. C. Johnson, and D. P. Chambers, 2014: Relative contributions of ocean mass and deep steric changes to sea level rise between 1993 and 2013. *J. Geophys. Res. Oceans*, **119**, 7509–7522, doi:10.1002/2014JC010180.

Ray, R. D., and B. C. Douglas, 2011: Experiments in reconstructing twentieth-century sea levels. *Prog. Oceanogr.*, **91**, 496–515, doi:10.1016/j.pocean.2011.07.021.

Reager, J. T., A. S. Gardner, J. S. Famiglietti, D. N. Wiese, A. Eicker, and M.-H. Lo, 2016: A decade of sea level rise slowed by climate-driven hydrology. *Science*, **351**, 699–703, doi:10.1126/science.aad8386.

Ritz, C., T. L. Edwards, G. Durand, A. J. Payne, V. Peyaud, and R. C. A. Hindmarsh, 2015: Potential sea-level rise from Antarctic ice-sheet instability constrained by observations. *Nature*, **528**, 115–118, doi:10.1038/nature16147.

Schmidt, G. A., and Coauthors, 2014: Configuration and assessment of the GISS ModelE2 contributions to the CMIP5 archive. *J. Adv. Model. Earth Syst.*, **6**, 141–184, doi:10.1002/2013MS000265.

Sen Gupta, A., N. C. Jourdain, J. N. Brown, and D. Monselesan, 2013: Climate drift in CMIP5 models. *J. Climate*, **26**, 8597–8615, doi:10.1175/JCLI-D-12-00521.1.

Shepherd, A., and Coauthors, 2012: A reconciled estimate of ice-sheet mass balance. *Science*, **338**, 1183–1189, doi:10.1126/science.1228102.

Slangen, A. B. A., M. Carson, C. A. Katsman, R. S. W. van de Wal, A. Koehl, L. L. A. Vermeersen, and D. Stammer, 2014a: Projecting twenty-first century regional sea-level changes. *Climatic Change*, **124**, 317–332, doi:10.1007/s10584-014-1080-9.

——, J. A. Church, X. Zhang, and D. Monselesan, 2014b: Detection and attribution of global mean thermosteric sea level change. *Geophys. Res. Lett.*, **41**, 5951–5959, doi:10.1002/2014GL061356.

——, ——, ——, and ——, 2015: The sea-level response to external forcings in CMIP5 climate models. *J. Climate*, **28**, 8521–8539, doi:10.1175/JCLI-D-15-0376.1.

——, ——, C. Agosta, X. Fettweis, B. Marzeion, and K. Richter, 2016: Anthropogenic forcing dominates global mean sea-level rise since 1970. *Nat. Climate Change*, **6**, 701–705, doi:10.1038/nclimate2991.

——, F. Adloff, S. Jevrejeva, P. W. Leclercq, B. Marzeion, Y. Wada, and R. Winkelmann, 2017: A review of recent updates of sea-level projections at global and regional scales. *Surv. Geophys.*, **38**, 385–406, doi:10.1007/s10712-016-9374-2.

Smith, D. M., and Coauthors, 2015: Earth's energy imbalance since 1960 in observations and CMIP5 models. *Geophys. Res. Lett.*, **42**, 1205–1213, doi:10.1002/2014GL062669.

Spada, G., 2017: Glacial isostatic adjustment and contemporary sea level rise: An overview. *Surv. Geophys.*, **38**, 153–185, doi:10.1007/s10712-016-9379-x.

Sutterley, T. C., I. Velicogna, E. Rignot, J. Mouginot, T. Flament, M. R. van den Broeke, J. M. van Wessem, and C. H. Reijmer, 2014: Mass loss of the Amundsen Sea Embayment of West Antarctica from four independent techniques. *Geophys. Res. Lett.*, **41**, 8421–8428, doi:10.1002/2014GL061940.

Tamisiea, M. E., 2011: Ongoing glacial isostatic contributions to observations of sea level change. *Geophys. J. Int.*, **186**, 1036–1044, doi:10.1111/j.1365-246X.2011.05116.x.

Taylor, K. E., R. J. Stouffer, and G. A. Meehl, 2012: An overview of CMIP5 and the experiment design. *Bull. Amer. Meteor. Soc.*, **93**, 485–498, doi:10.1175/BAMS-D-11-00094.1.

Thompson, P. R., B. D. Hamlington, F. W. Landerer, and S. Adhikari, 2016: Are long tide gauge records in the wrong place to measure global mean sea level rise? *Geophys. Res. Lett.*, **43**, 10 403–10 411, doi:10.1002/2016GL070552.

van Angelen, J. H., M. R. van den Broeke, B. Wouters, and J. T. M. Lenaerts, 2014: Contemporary (1960–2012) evolution of the climate and surface mass balance of the Greenland Ice Sheet. *Surv. Geophys.*, **35**, 1155–1174, doi:10.1007/s10712-013-9261-z.

Velicogna, I., T. C. Sutterley, and M. R. van den Broeke, 2014: Regional acceleration in ice mass loss from Greenland and Antarctica using GRACE time-variable gravity data. *Geophys. Res. Lett.*, **41**, 8130–8137, doi:10.1002/2014GL061052.

Voldoire, A., and Coauthors, 2013: The CNRM-CM5.1 global climate model: Description and basic evaluation. *Climate Dyn.*, **40**, 2091–2121, doi:10.1007/s00382-011-1259-y.

von Schuckmann, K., and Coauthors, 2016: An imperative to monitor Earth's energy imbalance. *Nat. Climate Change*, **6**, 138–144, doi:10.1038/nclimate2876.

Wada, Y., L. P. H. van Beek, F. C. Sperna Weiland, B. F. Chao, Y.- H. Wu, and M. F. P. Bierkens, 2012: Past and future contribution of global groundwater depletion to sea-level rise. *Geophys. Res. Lett.*, **39**, L09402, doi:10.1029/2012GL051230.

——, M.-H. Lo, P. J.-F. Yeh, J. T. Reager, J. S. Famiglietti, R.-J. Wu, and Y.-H. Tseng, 2016: Fate of water pumped from underground and contributions to sea-level rise. *Nat. Climate Change*, **6**, 777–780, doi:10.1038/nclimate3001.

——, J. T. Reager, B. F. Chao, J. Wang, M.-H. Lo, C. Song, Y. Li, and A. S. Gardner, 2017: Recent changes in land water storage and its contribution to sea level variations. *Surv. Geophys.*, **38**, 131–152, doi:10.1007/s10712-016-9399-6.

Watanabe, M., and Coauthors, 2010: Improved climate simulation by MIROC5: Mean states, variability, and climate sensitivity. *J. Climate*, **23**, 6312–6335, doi:10.1175/2010JCLI3679.1.

Watanabe, S., and Coauthors, 2011: MIROC-ESM: Model description and basic results of CMIP5-20c3m experiments. *Geosci. Model Dev.*, **4**, 845–872, doi:10.5194/gmdd-4-1063-2011.

Watson, C. S., N. J. White, J. A. Church, M. A. King, R. J. Burgette, and B. Legresy, 2015: Unabated global mean sea-level rise over the satellite altimeter era. *Nat. Climate Change*, **5**, 565–568, doi:10.1038/nclimate2635.

Yang, D., and O. A. Saenko, 2012: Ocean heat transport and its projected change in CanESM2. *J. Climate*, **25**, 8148–8163, doi:10.1175/JCLI-D-11-00715.1.

Yukimoto, S., and Coauthors, 2012: A new global climate model of the Meteorological Research Institute: MRI-CGCM3—Model description and basic performance. *J. Meteor. Soc. Japan*, **90A**, 23–64, doi:10.2151/jmsj.2012-A02.